Crouzeix-Velte Decompositions and the Stokes Problem

PhD Thesis

Györgyi Strauber

2008

Crouzeix-Velte Decompositions and the Stokes Problem

PhD Thesis

Györgyi Strauber

Thesis supervisor: Dr. Gisbert Stoyan

Professor, Eötvös Loránd University of Sciences, Faculty of Informatics,
Department of Numerical Analysis

Eötvös Loránd University of Sciences, Insitute of Mathematics,
Mathematical Doctoral School

Director of the Doctoral School: Dr. Miklós Laczkovich

Professor, Member of the Hungarian Academy of Sciences

Applied Mathematics Doctoral Program

Director of the program: Dr. Michaletzky György

Professor, Doctor of the Hungarian Academy of Sciences

This thesis was written at

Dunaújvárosi Főiskola

Dunaújváros, 2008

Contents

1 Introduction

In our dissertation the staggered grid approximation of the Stokes problem on several special domains and with different boundary conditions is investigated, moreover, several other Stokes-approximations are also considered. We deal with methods where the discrete Crouzeix-Velte decomposition exists: we prove the existence of this decomposition and show numerical results to prove the effectiveness of these discretizations.

The Crouzeix-Velte decomposition is a decomposition into three orthogonal subspaces of the customary Sobolev space $(H_0^1(\Omega))^n$ of vector functions defined over a lipschitzian domain $\Omega \subset \mathbb{R}^n$, $n = 2, 3$ which first has been described in [8] and later, independently, in [31]. This decomposition is similar to the well-known Helmholtz-Weyl decomposition (for vector functions belonging to $(L_2)^n$) but different from the latter; not only by the boundary conditions prescribed for the former (originally homogeneous Dirichlet conditions) but also by the properties of the functions in the three subspaces: for Helmholtz-Weyl decomposition the third subspace consists of vector functions which are both divergence- and rotationfree (i.e. harmonic) whereas for Crouzeix-Velte decomposition, along with the subspaces of divergence-free and rotation-free functions, there is a third subspace - the functions of which have both nonzero divergence and rotation or are the zero function (but all functions here are biharmonic).

In [31] and [9], the decomposition has been used to get more information about the inf-sup constant of the Stokes problem. The optimal inf-sup constant can be characterized by the third subspace alone [22].

For the numerical solution of the Stokes problem and its connection to the inf-sup problem, see [5], [14], [6]. In [7], additional results were gained about the inf-sup constant for ring and disk domains.

If using discretization methods for approximating the Stokes equations, and if the discrete scheme admits a discrete Crouzeix–Velte decomposition, then the same conclusions as in the continuous case can be drawn. The subspaces of the discrete rotation-free and discrete divergence-free functions are in similar relation as the corresponding subspaces of $(H_0^1)^n$, and there is a third orthogonal subspace consisting of discretely biharmonic functions. The optimal constant of the discrete inf-sup condition can therefore be computed on this much smaller third space.

These results are of interest for the iterative solution of stationary problems for the Stokes and linear elasticity equations, and for long-term calculations in the time-dependent case for the following reasons: if there exists a discrete Crouzeix-Velte decomposition, then independently of the domain and its triangulation, in the spectrum of the discrete Schur complement operator, there is an eigenvalue 1 of high multiplicity (of the order of inner grid points). Then, the error components lying in the eigensubspace corresponding to this eigenvalue can be removed by one step of a simple damped Jacobi iteration. The remaining error lies in an eigensubspace of much smaller dimension connected only with boundary effects. Moreover, the conjugate gradient iteration automatically takes advantage of such a spectrum and converges faster than for discrete spaces without a decomposition.

In [22] and [11], discrete and algebraic versions of the Crouzeix-Velte decomposition have been developed. Here, the discrete versions referred to the staggered grid approximation of the two- and three-dimensional Stokes problem and to conforming finite element approximations, especially to the high-order Scott-Vogelius elements.

In [23], the Uzawa and Arrow-Hurwitz iterations are investigated and are shown to reach the third Crouzeix–Velte subspace after at most 2 steps, and an improved convergence estimate is derived for the conjugate gradient method using the estimates of the inf-sup constant. A general investigation of algebraic Crouzeix-Velte decomposition is given in [24], and the dimension of the third subspace for Scott-Vogelius elements is estimated from below.

In [25], the Crouzeix-Velte decomposition is generalized in respect to boundary conditions and boundary value problems.

The outline of the dissertation is as follows. In Section 2, the necessary notations and the analytical, the algebraic and the discrete Crouzeix–Velte decomposition are introduced as well as the Stokes problem in a cartesian coordinate system is described.

In Section 3, the well-known staggered grid approximation of the Stokes-problem in 2D case, on a non-equidistant rectangular grid with homogeneous Dirichlet boundary conditions is investigated. It is shown that the discrete Crouzeix–Velte decomposition exists for the Shortley-Weller approximation only if the grid spacing is changing linearly. It is also shown that using the finite volume method on a rectangular grid, the discrete Crouzeix–Velte decomposition exists without any condition on the grid spacing. These results are done not only for rectangles but also for domains composed of rectangles.

Finally, we show some computational results. Here it becomes visible that – from the point of view of the convergence rate of Uzawa- and conjugate gradient-like methods for the iterative solution of the corresponding discrete Stokes problems – it is worth using non-equidistant grids. These results, except the Proof of Theorem 3, were published in [28].

In Section 4, we investigate the existence of the discrete Crouzeix–Velte decomposition, in the case of the second order finite difference method. Further we generalize the Crouzeix-Velte decomposition in respect to boundary conditions. The staggered grid approximation of the Stokes problem is considered in the case where the domain is the unit square subdivided by an equidistant grid, the generalized boundary conditions are periodical and special non-standard boundary conditions. It is shown, that the results on existence of an analytical Crouzeix–Velte decomposition for the Stokes problem along with these boundary conditions carry over to the discrete case for the staggered grid approximation. These results were published in [25] and in [28].

In Section 5, the staggered grid approximation of the Stokes-problem in 3D case is investigated and the existence of the discrete Crouzeix–Velte decomposition is proved. Here the domain is a brick subdivided by a rectangular grid and the boundary conditions are homogeneous Dirichlet and periodical boundary conditions. These results were not published before. Let us point out that, earlier, concerning the 3D case only the results in [11] were published.

In Section 6, the staggered grid approximation of the Stokes-problem is investigated in a polar coordinate system, and the existence of the discrete Crouzeix–Velte decomposition for the unit disk is proved, in the case of second order approximation and homogeneous Dirichlet boundary conditions. Further here computational results are presented, using the Uzawa algorithm (as outer iteration) and solving the discrete Poisson equations by the conjugate gradient method (as inner iteration) with an effective preconditioning matrix and FFT algorithm. The results show that the discretization obeying a discrete Crouzeix–Velte decomposition leads to effectively solvable systems of algebraic equations. The average number of the outer iterations using the Uzawa algorithm was 3-5, and the number of inner iterations needed to reach the stopping criterion of the conjugate gradient method, using the best preconditioning matrix, was only 2. These results were published in [29]. Also in this section we show additional, non yet published numerical results: we solve the discrete Poisson equations on the unit disk by the multigrid method, as inner iteration. We describe the restriction and prolongation operators and we compare several pre- and post-smoothing iterations. The optimal iteration parameter of the damped Jacobi iteration - as smoothing iteration - is also calculated. The results show that the Gauss-Seidel iteration combined with a block Gauss-Seidel iteration step is the most effective as smoothing iteration resulting similar speed of convergence as the conjugate gradient method, using the best preconditioning matrix.

2 Notations

2.1 The Stokes problem

A Stokes problem can be derived from Navier-Stokes equations, well known from flow theory, e.g. by semidiscretization, see [27]. In our dissertation we consider at first the following first-kind Stokes problem in a cartesian coordinate system:

$$\begin{aligned} -\Delta\vec{u} + \operatorname{grad} p &= \vec{f}, \text{ in } \Omega, & (2.1)\\ \operatorname{div}\vec{u} &= 0, \text{ in } \Omega, & (2.2) \end{aligned}$$

where Ω is a bounded, simply-connected open domain in $\mathbb{R}^n$, $n = 2, 3$ with Lipschitz – continuous boundary $\partial\Omega$, and

$$\vec{u}(x) = (u_1(x), \dots, u_n(x))^T, \ \vec{f}(x) = (f_1(x), \dots, f_n(x))^T$$

defined for $x = (x_1, \dots, x_n) \in \Omega$.

On the boundary, homogeneous Dirichlet boundary conditions are imposed:

$$\vec{u} = 0, \text{ on } \partial\Omega. \tag{2.3}$$

The problem consists in finding a vector-function $\vec{u}(x)$ and a scalar function $p(x)$ that satisfy the system of partial differential equations above. The function $\vec{u}$ is the velocity of fluid and p is the (kinematic) pressure. For a constant also appearing in the first equation, the kinematic viscosity, we have chosen the value 1. Finally, f describes accelerations caused by an external force field, and the boundary conditions mean that the walls are impermeable and at rest.

Here $\Delta\vec{u} = (\Delta u_1, \dots, \Delta u_n)^T$, where

$$\begin{aligned} \Delta &= \sum_{i=1}^{n} \frac{\partial^2}{\partial x_i^2} \text{ denotes the Laplace operator,}\\ \operatorname{div}\vec{u} &= \sum_{i=1}^{n} \frac{\partial u_i}{\partial x_i} \text{ the divergence and}\\ \operatorname{grad} p &= \left(\frac{\partial p}{\partial x_1}, \dots, \frac{\partial p}{\partial x_n}\right)^T \text{ the gradient.} \end{aligned} \tag{2.4}$$

A unique weak solution $\vec{u} \in V$ and $p \in P$ exists when, for example, $\vec{f} \in (L_2(\Omega))^n$, (see, e.g., [19],[30]), where $P := L_{2,0}(\Omega)$ is the subspace of

$L_2(\Omega)$ of square integrable functions with zero integral over Ω , with the Hilbert space

$$L_2(\Omega) = \{\phi | (\phi,\phi) < \infty\}, (\phi,\psi) = \int_\Omega \phi\psi d\Omega$$

and where $V := (H_0^1(\Omega))^n$ is the well-known Sobolev space, with generalized derivatives in $(L_2(\Omega))^n$ and with zero boundary values in the sense of traces on the boundary $\partial\Omega$, see [1].

The variational formulation of the Stokes problem above is the following:

$$\begin{aligned} a(\vec{u},\vec{v}) + b(\vec{v},p) &= (\vec{f},\vec{v}), \text{ for all } \vec{v} \in V, && (2.5)\\ b(\vec{u},q) &= 0, \text{ for all } q \in L_{2,0}(\Omega). && (2.6) \end{aligned}$$

where

$$\begin{aligned} (\vec{f},\vec{v}) &:= \sum_{i=1}^n (f_i, v_i) = \int_\Omega \sum_{i=1}^n f_i(x) v_i(x) dx, && (2.7)\\ a(\vec{u},\vec{v}) &:= \int_\Omega \sum_{i,j=1}^n \frac{\partial u_i}{\partial x_j}\frac{\partial v_i}{\partial x_j} dx, && (2.8)\\ b(\vec{u},p) &:= -(\operatorname{div}\vec{u},p). && (2.9) \end{aligned}$$

and the problem is - as previously - to find a velocity vector $\vec{u}(x) \in V$ and a pressure $p(x) \in L_{2,0}$.

It is well known (see [14], [6]) that the solution of this problem depends in a stable way on the data since for Lipschitz domains the so-called inf-sup condition is satisfied:

$$\sup_{u \neq 0} b^2(u,p)/a(u,u) \geq \beta_0^2 \|p\|^2 \quad \text{for all } 0 \neq p \in L_{2,0}; \quad \beta_0 = \beta_0(\Omega) > 0.$$

In our dissertation, we consider finite difference and finite volume methods for special domains; for the numerical solution by finite element methods (for general domains), see [14].

2.2 The Crouzeix–Velte decomposition

Using the notation (2.8) above, the following identity is well-known for any $w, v \in V$ in both the two- or three-dimensional case:

$$a(w,v) := (\operatorname{div} w, \operatorname{div} v) + (\operatorname{rot} w, \operatorname{rot} v). \tag{2.10}$$

In the three-dimensional case $\operatorname{rot} w$ is defined as usual and in the two-dimensional case $\operatorname{rot} w$ is defined as the scalar $\frac{\partial w_2}{\partial x_1} - \frac{\partial w_1}{\partial x_2}$ often also denoted by $\operatorname{curl} w$.

On the basis of (2.10), the following orthogonal decomposition of V was derived in [31],[8]:

$$(H_0^1(\Omega))^n = V = V_0 \oplus V_1 \oplus V_\beta, \tag{2.11}$$

where

$$\begin{aligned} V_0 &:= \ker \operatorname{div} = \{w \in V,\ \operatorname{div} w = 0\}, && (2.12)\\ V_1 &:= \ker \operatorname{rot} = \{w \in V,\ \operatorname{rot} w = 0\} && (2.13) \end{aligned}$$

and orthogonality is understood in the scalar product (2.8). The third orthogonal subspace V_β consists of biharmonic vector functions.

The space $L_2(\Omega)$ is decomposed similarly (see [22]) into three orthogonal subspaces:

$$L_2(\Omega) = P_0 \oplus P_1 \oplus P_\beta, \tag{2.14}$$

where

$$P_0 := \ker \operatorname{grad}, \quad P_1 = \operatorname{div} \ker \operatorname{rot} = \operatorname{div} V_1, \quad P_\beta = \operatorname{div} V_\beta. \tag{2.15}$$

Here orthogonality is understood in the sense of L_2 and P_0 is the one-dimensional space of functions constant on Ω, P_β consists of harmonic functions.

Both decompositions (2.11) and (2.14) are called *analytical* Crouzeix–Velte decompositions.

We next describe the *algebraic* Crouzeix–Velte decomposition of $\mathbb{R}^n$. For an $n > 2$, let $(\cdot,\cdot)$ denote the Euclidean scalar product in $\mathbb{R}^n$, moreover, let $A, B, C \in \mathbb{R}^{n\times n}$ be matrices satisfying

$$\begin{aligned} A &= B + C, && (2.16)\\ A &= A^T > 0, && (2.17)\\ B = B^T \geq 0 \quad &, \quad C = C^T \geq 0, && (2.18)\\ \delta := \dim\ker B \geq 1 \quad &, \quad \rho := \dim\ker C \geq 1. && (2.19) \end{aligned}$$

Then, with a suitable subspace $W \subset \mathbb{R}^n$ (which may turn out to be empty) and with orthogonality to be understood in the sense of the scalar product $(A\cdot,\cdot)$, the following orthogonal decomposition of $\mathbb{R}^n$ can be derived (see [24]):

$$\mathbb{R}^n = \ker B \oplus \ker C \oplus W. \tag{2.20}$$

For the eigenvalues λ_i of the generalized eigenvalue problem

$$\lambda A x = B x \tag{2.21}$$

we have

$$\lambda_i \in [0,1] \text{ for all } i \tag{2.22}$$

and also using the eigenvectors $x^{(i)}$, the subspaces in (2.20) can be characterized as follows:

$$\begin{array}{rcl} \ker B & = & span(x^{(i)}, \lambda_i = 0), \\ \ker C & = & span(x^{(i)}, \lambda_i = 1), \\ W & = & span(x^{(i)}, \lambda_i \in (0,1)). \end{array} \tag{2.23}$$

Decomposition (2.20) is an algebraic version of (2.11) due to the following correspondences connected with the matrices in (2.16):

$$A \sim -\Delta, \;\; B \sim -\operatorname{grad}\operatorname{div}, \;\; C \sim \operatorname{curl}\operatorname{rot},$$

where Δ is the (vector) Laplace operator and where the sign $\sim$ expresses only an analogy between a differential operator and a matrix, and is not necessarily a (good) approximation. In this sense (2.16) corresponds to the well known identity

$$-\Delta = -\operatorname{grad}\operatorname{div} + \operatorname{curl}\operatorname{rot} \tag{2.24}$$

of vector analysis.

The algebraic Crouzeix–Velte decomposition is *proper* in case $\dim W = n - \delta - \rho > 0$.

In the *discrete* case, the velocity space (which approximates $(H^1(\Omega))^n$ or a subspace of the latter) will be denoted by $\vec{V}_h$, the pressure space will be denoted by P_h, and div_h and rot_h will be written for the discrete equivalents of the divergence and rotation operator, Δ_h will denote the discrete Laplace operator. The matrix corresponding to the mapping $-\operatorname{div}_h$ from the velocity space into the pressure space is denoted by $\tilde{B}_h$ and we introduce the following notations: $\tilde{C}_h$ for the matrix of the operator rot_h and A_h for the matrix of the operator $-\Delta_h$. If A_h, $\tilde{B}_h$, $\tilde{C}_h$ matrices satisfy the following:

$$\begin{aligned} A_h &= B_h + C_h, \\ A_h &= A_h^T > 0, \end{aligned} \tag{2.25}$$

where $B_h = \tilde{B}_h^T \tilde{B}_h$ and $C_h = \tilde{C}_h^T \tilde{C}_h$ and $\ker \tilde{B}_h \neq \emptyset$ and $\ker \tilde{C}_h \neq \emptyset$, then a discrete Crouzeix-Velte decomposition exists and (2.20) takes the form

$$V_h = \ker \mathrm{div}_h \oplus \ker \mathrm{rot}_h \oplus W = V_{h,0} \oplus V_{h,1} \oplus V_{h,\beta}.$$

P_h is decomposed similarly into three orthogonal subspaces:

$$P_h = \ker \mathrm{grad}_h \oplus \mathrm{div}_h \ker \mathrm{rot}_h \oplus \mathrm{div}_h V_{h,\beta} = P_{h,0} \oplus P_{h,1} \oplus P_{h,\beta}.$$

After discretization by the finite element or finite difference methods, the Stokes problem takes the following form ([14],[28],[29]):

$$\begin{pmatrix} A_h & \tilde{B}_h^T \\ \tilde{B}_h & 0 \end{pmatrix} \begin{pmatrix} u \\ p \end{pmatrix} = \begin{pmatrix} f \\ 0 \end{pmatrix}. \tag{2.26}$$

Here A_h is a matrix of dimension $n_h \times n_h$, n_h denotes the number of velocity degrees of freedom; the 0 block is of dimension $m_h \times m_h$, with the number m_h of pressure degrees of freedom; $\tilde{B}_h$ is of dimension $m_h \times n_h$. Further, u, p and f denote the coefficient vectors of velocities and pressure and of the projection of the force vector, respectively.

With these matrices (2.21) corresponds to

$$\lambda_h A_h x_h = B_h x_h,$$

which is transformed by $p_h := \tilde{B}_h x_h$ into

$$\lambda_h p_h = S_h p_h,$$

where S_h is the discrete Schur complement operator of the Stokes problem, $S_h := \tilde{B}_h A_h^{-1} \tilde{B}_h^T$. If the discrete Crouzeix-Velte decomposition exists then $\lambda_h \in [0, 1]$ ([22]).

3 The staggered grid approximation on non-equidistant rectangular grids

First we consider the well-known staggered-grid approximation where Ω is a rectangle subdivided by a non-equidistant grid into $(n-1)(m-1)$ rectangular cells. (For the simplicity hereafter we deal with the case $n = m$, but our results hold if $n \neq m$ as well.) The cell midpoints are pressure nodes, the pressure vector is denoted by p_h and its components by p_{ij}, with $i, j = 1, \ldots, n-1$. The area of the cell of p_{ij} is $h_{1,i+1/2}h_{2,j+1/2}$, where $h_{1,i+1/2}$ is the length of the north-south sides of the cell and $h_{2,j+1/2}$ is the length of the east-west sides. The sides of the cells contain as their midpoints the velocity nodes: nodes of the u-components of the velocity are on the east-west sides, nodes of the v-components are on the north-south sides, and there are $(n-1)n$ such nodes of each velocity component (including the boundary nodes). The velocity components are denoted by u_{ij}, $i = 1, \ldots, n$, $j = 1, \ldots, n-1$, and by v_{ij}, $i = 1, \ldots, n-1$, $j = 1, \ldots, n$. Here the u_{ij} with $i = 1$ and $i = n$ are the boundary values of u_h; the v_{ij} with $j = 1$ and $j = n$ are the boundary values of v_h. The staggered grid approximation is shown on Figure 1. The space $\mathbb{R}^{m_h}$ will be called the pressure space and denoted by P_h; and the space $\mathbb{R}^{n_h}$ is the velocity space and it is denoted by $\vec{V}_h$, where $m_h := (n-1)^2$ and $n_h := 2(n-2)(n-1)$ — taking into account that the boundary values of the velocity components are zero.

For the approximation of the Stokes problem we need the discrete divergence operator (the used grid points are illustrated with red colour) and the discrete vector Laplace operator (marked with blue). Moreover, we will define also the discrete rotation operator (marked with green).

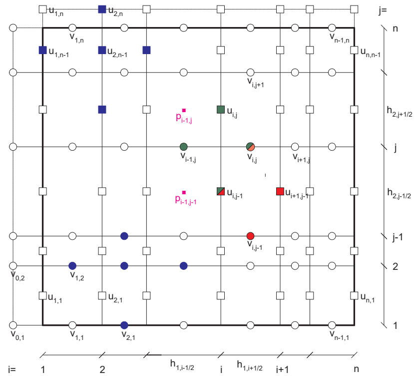

Figure 1: Staggered grid approximation on a non-equidistant rectangular grid

3.1 The finite difference approximation on a staggered grid

First we use the finite difference method to approximate the Stokes problem on the staggered grid. To simplify the expressions, the following notations will be introduced:

$$
\begin{aligned}
\tilde{h}_{1,i+1/2} &:= \frac{h_{1,i-1/2} + 2h_{1,i+1/2} + h_{1,i+3/2}}{4} \\
\tilde{h}_{2,j+1/2} &:= \frac{h_{2,j-1/2} + 2h_{2,j+1/2} + h_{2,j+3/2}}{4} \\
\tilde{h}_{1,i} &:= \frac{h_{1,i-1/2} + h_{1,i+1/2}}{2} \\
\tilde{h}_{2,j} &:= \frac{h_{2,j-1/2} + h_{2,j+1/2}}{2}
\end{aligned}
$$

For pressure vectors p_h, q_h and velocity vectors $\vec{u}_h = (u_h, v_h)^T$, $\vec{w}_h = (r_h, s_h)^T$ the following discrete scalar products and the corresponding norms are introduced:

$$
\begin{aligned}
(p_h, q_h)_{0,h} &:= \sum_{i,j=1}^{n-1} p_{ij} q_{ij} h_{1,i+1/2} h_{2,j+1/2}, \\
\|p_h\|_{0,h}^2 &:= (p_h, p_h)_{0,h},
\end{aligned}
\tag{3.1}
$$

and

$$
\begin{aligned}
(p_h, q_h)_{0,\tilde{h}} &:= \sum_{i=1}^{n-2} \sum_{j=1}^{n} p_{ij} q_{ij} \tilde{h}_{1,i+1} \tilde{h}_{2,j} + \\
&+ \sum_{j=2}^{n-1} p_{0,j} q_{0,j} \tilde{h}_{1,1} \tilde{h}_{2,j} + \sum_{j=2}^{n-1} p_{n-1,j} q_{n-1,j} \tilde{h}_{1,n} \tilde{h}_{2,j}, \\
\|p_h\|_{0,\tilde{h}}^2 &:= (p_h, p_h)_{0,\tilde{h}},
\end{aligned}
\tag{3.2}
$$

moreover

$$
\begin{aligned}
(\vec{u}_h, \vec{w}_h)_{0,h} &:= \sum_{i=2}^{n-1} \sum_{j=1}^{n-1} u_{ij} r_{ij} \tilde{h}_{1,i} \tilde{h}_{2,j+1/2} + \\
&\qquad + \sum_{i=1}^{n-1} \sum_{j=2}^{n-1} v_{ij} s_{ij} \tilde{h}_{1,i+1/2} \tilde{h}_{2,j}, \\
\|\vec{u}_h\|_{0,h}^2 &:= (\vec{u}_h, \vec{u}_h)_{0,h}.
\end{aligned}
\tag{3.3}
$$

The pressure space P_h with the scalar product (3.1) and corresponding norm becomes a Hilbert space; similarly, the velocity space $\vec{V}_h$, with the scalar product (3.3) is also a Hilbert space.

The divergence is approximated as follows:

$$
(\operatorname{div}_h \vec{u}_h)_{ij} := \frac{u_{i+1,j} - u_{ij}}{h_{1,i+1/2}} + \frac{v_{i,j+1} - v_{ij}}{h_{2,j+1/2}}, \tag{3.4}
$$

where $\vec{u}_h := (u_h, v_h)^T$ and $i = 1, \ldots, n-1,\ j = 1, \ldots, n-1$. The matrix corresponding to the mapping $-\operatorname{div}_h$ from the velocity space into the pressure space is denoted by $\tilde{B}_h$. For the approximation of the discrete Laplace operator we continue the grid by two lines for u-nodes: one above the square at a distance $h_{2,n+1/2}/2$ and one below the square at a distance $h_{2,1/2}/2$. Further we continue the grid by two lines for v-nodes: one left to the square at a distance $h_{1,1/2}/2$ and one right to the square at a distance $h_{1,n+1/2}/2$. Putting zero values into the u- or v-nodes on these lines and using the usual Shortley-Weller approximation for the discrete Laplace operator (see, e.g., [27]) in all inner velocity nodes, we get the following first order approximation:

$$\begin{aligned}
\Delta_h \vec{u}_h &= (\Delta_h u_h, \Delta_h v_h)^T, \\
(\Delta_h u_h)_{ij} &:= \frac{1}{\tilde{h}_{1,i}} \left(\frac{u_{i+1,j} - u_{ij}}{h_{1,i+1/2}} - \frac{u_{ij} - u_{i-1,j}}{h_{1,i-1/2}} \right) + \\
& \quad + \frac{1}{\tilde{h}_{2,j+1/2}} \left(\frac{u_{i,j+1} - u_{ij}}{\tilde{h}_{2,j+1}} - \frac{u_{ij} - u_{i,j-1}}{\tilde{h}_{2,j}} \right), \\
& \quad 2 \le i \le n-1, \;\; 1 \le j \le n-1, \\
(\Delta_h v_h)_{ij} &:= \frac{1}{\tilde{h}_{1,i+1/2}} \left(\frac{v_{i+1,j} - v_{ij}}{\tilde{h}_{1,i+1}} - \frac{v_{ij} - v_{i-1,j}}{\tilde{h}_{1,i}} \right) + \\
& \quad + \frac{1}{\tilde{h}_{2,j}} \left(\frac{v_{i,j+1} - v_{ij}}{h_{2,j+1/2}} - \frac{v_{ij} - v_{i,j-1}}{h_{2,j-1/2}} \right), \\
& \quad 1 \le i \le n-1, \;\; 2 \le j \le n-1.
\end{aligned} \tag{3.5}$$

The matrix corresponding to the mapping $-\Delta_h$ from the velocity space into itself is denoted by A_h. Finally, we define the discrete rotation as follows:

$$(\mathrm{rot}_h \, \vec{u}_h)_{ij} := \frac{v_{i+1,j} - v_{ij}}{\tilde{h}_{1,i+1}} - \frac{u_{i+1,j} - u_{i+1,j-1}}{\tilde{h}_{2,j}}, \tag{3.6}$$

and we use the following notation: $\tilde{C}_h$ for the matrix of the operator rot_h.

Theorem 1

$$(A_h \vec{u}_h, \vec{u}_h)_{0,h} = \|\tilde{B}_h \vec{u}_h\|^2_{0,h} + \|\tilde{C}_h \vec{u}_h\|^2_{0,\tilde{h}} \tag{3.7}$$

holds for all vectors $\vec{u}_h := (u_h, v_h)^T \in \vec{V}_h$ if and only if

$$h_{1,i+1/2} = \frac{h_{1,i-1/2} + h_{1,i+3/2}}{2}$$

and

$$h_{2,j+1/2} = \frac{h_{2,j-1/2} + h_{2,j+3/2}}{2}.$$

Proof. We continue the grid functions u_h and v_h by zero onto the grid of the whole two-dimensional plane and then we apply partial summation to

$(A_h\vec{u}_h, \vec{u}_h)_{0,h}$ and extend the summation in all expressions to all integer i, j. Then we get:

$$
\begin{aligned}
(A_h\vec{u}_h, \vec{u}_h)_{0,h} &= \sum_{i,j}(\frac{u_{i+1,j} - u_{ij}}{h_{1,i+1/2}})^2 h_{1,i+1/2}\tilde{h}_{2,j+1/2} + \\
&+ \sum_{i,j}(\frac{u_{i,j+1} - u_{ij}}{\tilde{h}_{2,j+1}})^2 \tilde{h}_{1,i}\tilde{h}_{2,j+1} + \\
&+ \sum_{i,j}(\frac{v_{i+1,j} - v_{ij}}{\tilde{h}_{1,i+1}})^2 \tilde{h}_{1,i+1}\tilde{h}_{2,j} + \\
&+ \sum_{i,j}(\frac{v_{i,j+1} - v_{ij}}{h_{2,j+1/2}})^2 h_{2,j+1/2}\tilde{h}_{1,i+1/2} \\
&= \sum_{i,j}\left(\frac{\tilde{h}_{2,j+1/2}}{h_{1,i+1/2}}(u_{i+1,j} - u_{ij})^2 + \frac{\tilde{h}_{1,i}}{\tilde{h}_{2,j+1}}(u_{i,j+1} - u_{ij})^2 + \right. \\
&\qquad \left. + \frac{\tilde{h}_{2,j}}{\tilde{h}_{1,i+1}}(v_{i+1,j} - v_{ij})^2 + \frac{\tilde{h}_{1,i+1/2}}{h_{2,j+1/2}}(v_{i,j+1} - v_{ij})^2\right).
\end{aligned}
$$

$\|\tilde{B}_h\vec{u}_h\|^2_{0,h}$ may be written as follows:

$$
\begin{aligned}
\|\tilde{B}_h\vec{u}_h\|^2_{0,h} &= \sum_{i,j}\left(\frac{u_{i+1,j} - u_{ij}}{h_{1,i+1/2}} + \frac{v_{i,j+1} - v_{ij}}{h_{2,j+1/2}}\right)^2 h_{1,i+1/2}h_{2,j+1/2} \\
&= \sum_{i,j}\left(\frac{h_{2,j+1/2}}{h_{1,i+1/2}}(u_{i+1,j} - u_{ij})^2 + \frac{h_{1,i+1/2}}{h_{2,j+1/2}}(v_{i,j+1} - v_{ij})^2 + \right. \\
&\qquad \left. + 2(u_{i+1,j} - u_{ij})(v_{i,j+1} - v_{ij})\right).
\end{aligned}
$$

$\|\tilde{C}_h\vec{u}_h\|^2_{0,\tilde{h}}$ can be written as

$$
\begin{aligned}
\|\tilde{C}_h\vec{u}_h\|^2_{0,\tilde{h}} &= \sum_{i,j}\left(\frac{-(u_{i+1,j} - u_{i+1,j-1})}{\tilde{h}_{2,j}} + \frac{v_{i+1,j} - v_{ij}}{\tilde{h}_{1,i+1}}\right)^2 \tilde{h}_{1,i+1}\tilde{h}_{2,j} \\
&= \sum_{i,j}\left(\frac{\tilde{h}_{1,i+1}}{\tilde{h}_{2,j}}(u_{i+1,j} - u_{i+1,j-1})^2 + \frac{\tilde{h}_{2,j}}{\tilde{h}_{1,i+1}}(v_{i+1,j} - v_{ij})^2 - \right. \\
&\qquad \left. - 2(u_{i+1,j} - u_{i+1,j-1})(v_{i+1,j} - v_{ij})\right).
\end{aligned}
$$

Performing some index shifts we get:

$$
\begin{aligned}
2\sum_{i,j}(u_{i+1,j} - u_{ij})(v_{i,j+1} - v_{ij}) &= \\
&= 2\sum_{i,j}(u_{i+1,j}v_{i,j+1} - u_{i+1,j}v_{ij} - u_{ij}v_{i,j+1} + u_{ij}v_{ij}) \\
&= 2\sum_{i,j}(u_{i+1,j-1}v_{ij} - u_{i+1,j}v_{ij} - u_{i+1,j-1}v_{i+1,j} + u_{i+1,j}v_{i+1,j}) \\
&= 2\sum_{i,j}(u_{i+1,j} - u_{i+1,j-1})(v_{i+1,j} - v_{ij}).
\end{aligned}
$$

Namely, to get from the second to the third line in the above formulae, in the fourth term we have replaced i by $i+1$, in the first term j by $j-1$, and in the third term both indices have been shifted. Applying both shifts also to the expression $\sum_{i,j}(u_{i,j+1} - u_{ij})^2$ in $(A_h\vec{u}_h, \vec{u}_h)_{0,h}$, we find

$$
\begin{aligned}
(A_h\vec{u}_h, \vec{u}_h)_{0,h} - \|\tilde{B}_h\vec{u}_h\|^2_{0,h} - \|\tilde{C}_h\vec{u}_h\|^2_{0,\tilde{h}} &= \\
= \sum_{i,j}\Big(&\frac{h_{2,j-1/2} - 2h_{2,j+1/2} + h_{2,j+3/2}}{4h_{1,i+1/2}}(u_{i+1,j} - u_{i,j})^2 + \\
&+ \frac{h_{1,i-1/2} - 2h_{1,i+1/2} + h_{1,i+3/2}}{4h_{2,j+1/2}}(v_{i,j+1} - v_{ij})^2\Big).
\end{aligned}
$$

Using the assumptions on the step lengths, we get

$$
(A_h\vec{u}_h, \vec{u}_h)_{0,h} - \|\tilde{B}_h\vec{u}_h\|^2_{0,h} - \|\tilde{C}_h\vec{u}_h\|^2_{0,\tilde{h}} = 0. \quad \bullet
$$

Remark 1. It can be shown that $\dim(V_{h0}) = (n-2)^2$, $\dim(V_{h1}) = (n-3)^2$ and $\dim(V_{h,\beta}) = 4n-9$, where n denotes the number of grid points (including corner points) along a side of the square. Namely, to compute $\dim(V_{h0}) = \dim\ker\operatorname{div}_h$ we count the number of conditions to get $\|\operatorname{div}_h\vec{u}_h\|^2_{0,h} = 0$. Excluding the very last cell (which is depending on the other cells) we have to require $\operatorname{div}_h\vec{u}_h = 0$ in all remaining cells, that is, in $(n-1)^2 - 1$ points. Then $\dim\ker\operatorname{div}_h = n_h - ((n-1)^2 - 1) = (n-2)^2$ where $n_h = 2(n-1)(n-2)$ denotes the number of velocity degrees of freedom. Similarly, to compute $\dim(V_{h1}) = \dim\ker\operatorname{rot}_h$ we count the number of conditions to get $\|\operatorname{rot}_h\vec{u}_h\|^2_{0,h} = 0$, starting from the boundary of the grid and proceeding to the center. Excluding the corners of the square and the very last cell corner in the center of the grid, in all other cell corners we have to require $\operatorname{rot}_h\vec{u}_h = 0$, that is in $n^2 - 5$ points. Then $\dim\ker\operatorname{rot}_h = n_h - (n^2 - 5) = (n-3)^2$. Therefore $\dim(V_{h,\beta}) = n_h - (n-2)^2 - (n-3)^2 = 4n - 9$.

(We remark that basis functions for $\ker \mathrm{rot}_h$ and $\ker \mathrm{div}_h$ have been described in [15], and for $\ker \mathrm{div}_h$ also in [10] and [6].) $\bullet$

Remark 2. Although A_h is not a symmetric matrix, it is symmetric in the sense of the scalar product (3.3). This means that (3.7) can be described in matrix terms as follows:

$$\begin{aligned}(D_A A_h \vec{u}_h, \vec{u}_h) &= (D_B \tilde{B}_h \vec{u}_h, \tilde{B}_h \vec{u}_h) + (D_C \tilde{C}_h \vec{u}_h, \tilde{C}_h \vec{u}_h) = \\ &= (\tilde{B}_h^T D_B \tilde{B}_h \vec{u}_h, \vec{u}_h) + (\tilde{C}_h^T D_C \tilde{C}_h \vec{u}_h, \vec{u}_h). \end{aligned} \tag{3.8}$$

where $(.,.)$ is the Euclidean scalar product and D_A, D_B, D_C are diagonal matrices corresponding to (3.3), (3.1) and (3.2):

$$\begin{aligned}
(D_A u_h)_k &= u_{i,j} \tilde{h}_{1,i} \tilde{h}_{2,j+1/2}, \\
k = (n-1)(i-2)+j, &\qquad 2 \le i \le n-1, 1 \le j \le n-1, \\
(D_A v_h)_k &= v_{i,j} \tilde{h}_{1,i+1/2} \tilde{h}_{2,j}, \\
k = (n-2)(i-1)+j-1, &\qquad 1 \le i \le n-1, 2 \le j \le n-1, \\
(D_B p_h)_k &= p_{i,j} h_{1,i+1/2} h_{2,j+1/2}, \\
k = (n-1)(i-1)+j, &\qquad 1 \le i, j \le n-1, \\
(D_C p_h)_k &= p_{i,j} \tilde{h}_{1,i+1} \tilde{h}_{2,j}, \\
k = n-2+n(i-1)+j, &\qquad 1 \le i \le n-2, 1 \le j \le n; \\
k = j-1, &\qquad i = 0, 2 \le j \le n-1; \\
k = (n-2)(n+1)+j-1, &\qquad i = n-1, 2 \le j \le n-1.
\end{aligned}$$

From (3.8) we get:

$$D_A A_h = \tilde{B}_h^T D_B \tilde{B}_h + \tilde{C}_h^T D_C \tilde{C}_h. \tag{3.9}$$

It follows that $D_A A_h$ is a symmetric matrix and can be written in the following form:

$$D_A A_h =: \hat{A}_h = B_h + C_h, \tag{3.10}$$

where $B_h = \hat{B}^T \hat{B}$ and $C_h = \hat{C}^T \hat{C}$ with the notation $\hat{B} = D_B^{1/2} \tilde{B}_h, \hat{C} = D_C^{1/2} \tilde{C}_h$.

Using the staggered grid approximation based on the finite volume method (see the following subsection) we get similarly:

$$D_{\underline{A}} A_{\underline{h}} = \tilde{B}_h^T D_B \tilde{B}_h + \tilde{C}_h^T D_C \tilde{C}_h. \tag{3.11}$$

where the diagonal matrix $D_{\underline{A}}$ corresponds to the scalar product (3.18).

Let us mention that using finite element methods - if the discrete Crouzeix–Velte decomposition exists - we can get the following:

$$A_h = \tilde{B}_h^T M_h^{-1} \tilde{B}_h + \tilde{C}_h^T M_h^{-1} \tilde{C}_h. \tag{3.12}$$

where M_h is the mass matrix (see [11]). $\bullet$

Remark 3. We have to show also that $D_A A_h = \hat{A}_h$ matrix is positive definite, that is $\hat{A}_h > 0$. This proof is the same as the proof of theorem 3, see in the next subsection. Together with remark 1 and 2, it means that a proper Crouzeix–Velte decomposition of the velocity and the pressure space into three nontrivial parts exists, if $n > 3$ (see [24]). $\bullet$

3.2 The staggered grid approximation based on the finite volume method

Now we use the finite volume method (sometimes also called box method) to approximate the Stokes problem ([17]). We start from the same staggered grid like in the preceding subsection, but for the approximation of $(\Delta_{\underline{h}} u_h)_{ij}$ we choose another subdivision, $\Omega = \cup \Omega_{ij}$ of Ω, where the midpoint of the rectangular cell, Ω_{ij} is u_{ij}. The expression (Δu) is integrated over Ω_{ij} and the Gauss-Ostrogradskij formula is used for transformation of the second order derivatives:

$$\int_{\Omega_{ij}} \mathrm{div}(\mathrm{grad}\, u) dx_1 dx_2 = \int_{\Gamma_{ij}} (\mathrm{grad}\, u) \vec{n} ds = \sum_{k=1}^{4} \vec{n}_k \int_{\gamma_k} (\mathrm{grad}\, u) ds, \quad (3.13)$$

where n is the normal vector of Γ_{ij}. Using suitable low order quadrature formulae for approximation of the integrals in (3.13), $(\Delta_{\underline{h}} u_h)_{ij}$ may be written as follows:

$$\begin{aligned}
(\Delta_{\underline{h}} u_h)_{ij} &= \Bigg(\frac{-(u_{ij} - u_{i,j-1})}{\tilde{h}_{2,j}} \tilde{h}_{1,i} + \frac{u_{i+1,j} - u_{ij}}{h_{1,i+1/2}} h_{2,j+1/2} + \qquad (3.14) \\
&\quad + \frac{u_{i,j+1} - u_{ij}}{\tilde{h}_{2,j+1}} \tilde{h}_{1,i} - \frac{u_{ij} - u_{i-1,j}}{h_{1,i-1/2}} h_{2,j+1/2} \Bigg) \frac{1}{h_{2,j+1/2}} \frac{1}{\tilde{h}_{1,i}} \\
&= \frac{1}{\tilde{h}_{1,i}} \left(\frac{u_{i+1,j} - u_{ij}}{h_{1,i+1/2}} - \frac{u_{ij} - u_{i-1,j}}{h_{1,i-1/2}} \right) + \\
&\quad + \frac{1}{h_{2,j+1/2}} \left(\frac{u_{i,j+1} - u_{ij}}{\tilde{h}_{2,j+1}} - \frac{u_{ij} - u_{i,j-1}}{\tilde{h}_{2,j}} \right), \\
&\quad 2 \le i \le n-1, \;\; 1 \le j \le n-1, \qquad (3.15)
\end{aligned}$$

For approximation of $(\Delta_{\underline{h}} v_h)_{ij}$ the domain Ω is subdivided in a different way. In this case the midpoint of Ω_{ij} sub-domain is v_{ij}. Similar to (3.14) we get:

$$\begin{aligned}
(\Delta_{\underline{h}} v_h)_{ij} &:= \frac{1}{h_{1,i+1/2}} \left(\frac{v_{i+1,j} - v_{ij}}{\tilde{h}_{1,i+1}} - \frac{v_{ij} - v_{i-1,j}}{\tilde{h}_{1,i}} \right) + \qquad (3.16) \\
&\quad + \frac{1}{\tilde{h}_{2,j}} \left(\frac{v_{i,j+1} - v_{ij}}{h_{2,j+1/2}} - \frac{v_{ij} - v_{i,j-1}}{h_{2,j-1/2}} \right), \\
&\quad 1 \le i \le n-1, \;\; 2 \le j \le n-1.
\end{aligned}$$

and

$$\Delta_{\underline{h}}\vec{u}_h = (\Delta_{\underline{h}} u_h, \Delta_{\underline{h}} v_h)^T \tag{3.17}$$

is the discrete vector Laplace operator. For approximation of $(\mathrm{div}_h\,\vec{u}_h)_{ij}$ we use the subdivision of Ω which is determined by the original grid and for $(\mathrm{rot}_h\,\vec{u}_h)_{ij}$ another subdivision where the midpoint of Ω_{ij} is a grid point of the original grid. Integrating the corresponding equations over Ω_{ij} and using suitable quadrature formulae we get the same approximation for $(\mathrm{div}_h\,\vec{u}_h)_{ij}$ and $(\mathrm{rot}_h\,\vec{u}_h)_{ij}$ as in (3.4) and (3.6). Instead of (3.3) we introduce the scalar product and corresponding norm as follows:

$$\begin{aligned}(\vec{u}_h, \vec{w}_h)_{0,h^*} \;&:=\; \sum_{i=2}^{n-1}\sum_{j=1}^{n-1} u_{ij} r_{ij} \tilde{h}_{1,i} h_{2,j+1/2} + \qquad (3.18)\\ &\quad + \sum_{i=1}^{n-1}\sum_{j=2}^{n-1} v_{ij} s_{ij} h_{1,i+1/2} \tilde{h}_{2,j},\\ \|\vec{u}_h\|^2_{0,h^*} \;&:=\; (\vec{u}_h, \vec{u}_h)_{0,h^*}. \qquad (3.19)\end{aligned}$$

Using the scalar products and norms (3.1), (3.2) and (3.18), and the approximations (3.14), (3.16), (3.4) and (3.6), we obtain:

Theorem 2.

$$(A_{\underline{h}}\vec{u}_h, \vec{u}_h)_{0,h^*} = \|\tilde{B}_h\vec{u}_h\|^2_{0,h} + \|\tilde{C}_h\vec{u}_h\|^2_{0,\tilde{h}}.$$

where $A_{\underline{h}}$ is defined as $-\Delta_{\underline{h}}$ and $\tilde{B}_h$, $\tilde{C}_h$ are the same as in Theorem 1.

Proof. Similarly to the proof of Theorem 1 we continue the grid functions u_h and v_h by zero onto the whole plane and then apply partial summation to $(A_{\underline{h}}\vec{u}_h, \vec{u}_h)_{0,h^*}$. Then there follows:

$$\begin{aligned}
(A_{\underline{h}}\vec{u}_h, \vec{u}_h)_{0,h^*} &= \sum_{i,j}\left(\frac{u_{i+1,j}-u_{ij}}{h_{1,i+1/2}}\right)^2 h_{1,i+1/2}h_{2,j+1/2} + \\
&\quad + \sum_{i,j}\left(\frac{u_{i,j+1}-u_{ij}}{\tilde{h}_{2,j+1}}\right)^2 \tilde{h}_{1,i}\tilde{h}_{2,j+1} + \\
&\quad + \sum_{i,j}\left(\frac{v_{i+1,j}-v_{ij}}{\tilde{h}_{1,i+1}}\right)^2 \tilde{h}_{1,i+1}\tilde{h}_{2,j} + \\
&\quad + \sum_{i,j}\left(\frac{v_{i,j+1}-v_{ij}}{h_{2,j+1/2}}\right)^2 h_{2,j+1/2}h_{1,i+1/2} \\
&= \sum_{i,j}\Big(\frac{h_{2,j+1/2}}{h_{1,i+1/2}}(u_{i+1,j}-u_{ij})^2 + \frac{\tilde{h}_{1,i}}{\tilde{h}_{2,j+1}}(u_{i,j+1}-u_{ij})^2 + \\
&\quad + \frac{\tilde{h}_{2,j}}{\tilde{h}_{1,i+1}}(v_{i+1,j}-v_{ij})^2 + \frac{h_{1,i+1/2}}{h_{2,j+1/2}}(v_{i,j+1}-v_{ij})^2\Big).
\end{aligned}$$

The further steps of the proof are the same as in the proof of Theorem 1. •

Theorem 3.

$\hat{A}_{\underline{h}} := D_{\underline{A}}A_{\underline{h}}$ is a positive definite matrix.

where $D_{\underline{A}}$ is a diagonal matrix corresponding to (3.18), that is

$$\begin{aligned}
(D_{\underline{A}}u_h)_{k,k} &= u_{i,j}\tilde{h}_{1,i}h_{2,j+1/2}, \\
k = (n-1)(i-2)+j, &\qquad 2 \le i \le n-1, 1 \le j \le n-1, \\
(D_{\underline{A}}v_h)_{k,k} &= v_{i,j}h_{1,i+1/2}\tilde{h}_{2,j}, \\
k = (n-2)(i-1)+j-1, &\qquad 1 \le i \le n-1, 2 \le j \le n-1.
\end{aligned}$$

Proof. From (3.14) and (3.16), using homogeneous Dirichlet boundary conditions:

$$\begin{array}{lll}
u_{i,j} = u_{n,j} = 0 & v_{0,j} = v_{n,j} = 0 & 1 \le j \le n-1 \\
v_{i,1} = v_{i,n} = 0 & u_{i,0} = u_{i,n} = 0 & 1 \le i \le n-1
\end{array}$$

we get:

$$
\begin{aligned}
(A_{\underline{h}}\vec{u}_h, \vec{u}_h)_{0,h^*} &= \sum_{i=1}^{n-1}\sum_{j=0}^{n-1}\left(\frac{u_{i+1,j}-u_{ij}}{h_{1,i+1/2}}\right)^2 h_{1,i+1/2}h_{2,j+1/2} + \\
&+ \sum_{i=1}^{n-1}\sum_{j=0}^{n-1}\left(\frac{u_{i,j+1}-u_{ij}}{\tilde{h}_{2,j+1}}\right)^2 \tilde{h}_{1,i}\tilde{h}_{2,j+1} + \\
&+ \sum_{i=0}^{n-1}\sum_{j=1}^{n-1}\left(\frac{v_{i+1,j}-v_{ij}}{\tilde{h}_{1,i+1}}\right)^2 \tilde{h}_{1,i+1}\tilde{h}_{2,j} + \\
&+ \sum_{i=0}^{n-1}\sum_{j=1}^{n-1}\left(\frac{v_{i,j+1}-v_{ij}}{h_{2,j+1/2}}\right)^2 h_{2,j+1/2}h_{1,i+1/2}.
\end{aligned} \tag{3.20}
$$

Since $u_{1,j} = 0$, we can write $u_{i+1,j}$ in the following form (see also the proof of the discrete embedding theorems in[26]: in what follows, we essentially repeat the proof of [26], for completeness and because our notations differ):

$$
u_{i+1,j} = \sum_{k=1}^{i} \frac{u_{k+1,j}-u_{kj}}{h_{1,k+1/2}} h_{1,k+1/2} \tag{3.21}
$$

Further, since $u_{n,j} = 0$:

$$
-u_{i+1,j} = \sum_{k=i+1}^{n-1} \frac{u_{k+1,j}-u_{kj}}{h_{1,k+1/2}} h_{1,k+1/2} \tag{3.22}
$$

Using the Cauchy-inequality from (3.21) we get:

$$
\begin{aligned}
u_{i+1,j}^2 &\le \sum_{l=1}^{i} h_{1,l+1/2} \sum_{k=1}^{i}\left(\frac{u_{k+1,j}-u_{kj}}{h_{1,k+1/2}}\right)^2 h_{1,k+1/2} = \\
&= x_{i+1}\sum_{k=1}^{i}\left(\frac{u_{k+1,j}-u_{kj}}{h_{1,k+1/2}}\right)^2 h_{1,k+1/2},
\end{aligned} \tag{3.23}
$$

since

$$
\sum_{l=1}^{i} h_{1,l+1/2} = x_{i+1}.
$$

Similarly from (3.22) we get:

$$\begin{aligned} u_{i+1,j}^2 &\leq \sum_{l=i+1}^{n-1} h_{1,l+1/2} \sum_{k=i+1}^{n-1} \left(\frac{u_{k+1,j} - u_{kj}}{h_{1,k+1/2}} \right)^2 h_{1,k+1/2} = \\ &= (1 - x_{i+1}) \sum_{k=i+1}^{n-1} \left(\frac{u_{k+1,j} - u_{kj}}{h_{1,k+1/2}} \right)^2 h_{1,k+1/2}, \end{aligned} \tag{3.24}$$

Multiplying (3.23) by $(1 - x_{i+1})$ and (3.24) by x_{i+1} the following inequality is obtained:

$$u_{i+1,j}^2 \leq x_{i+1}(1 - x_{i+1}) \sum_{k=1}^{n-1} \left(\frac{u_{k+1,j} - u_{kj}}{h_{1,k+1/2}} \right)^2 h_{1,k+1/2} \tag{3.25}$$

We multiply (3.25) by $h_{2,j+1/2}$ and sum over j:

$$\begin{aligned} &\sum_{j=0}^{n-1} u_{i+1,j}^2 h_{2,j+1/2} \leq \\ &x_{i+1}(1 - x_{i+1}) \sum_{j=0}^{n-1} \sum_{k=1}^{n-1} \left(\frac{u_{k+1,j} - u_{kj}}{h_{1,k+1/2}} \right)^2 h_{1,k+1/2} h_{2,j+1/2}. \end{aligned} \tag{3.26}$$

Finally we multiply (3.26) by $\tilde{h}_{1,i+1}$ and sum over i:

$$\begin{aligned} &\sum_{i=1}^{n-2} \left(\sum_{j=0}^{n-1} u_{i+1,j}^2 h_{2,j+1/2} \right) \tilde{h}_{1,i+1} \leq \\ &\leq \sum_{j=0}^{n-1} \sum_{k=1}^{n-1} \left(\frac{u_{k+1,j} - u_{kj}}{h_{1,k+1/2}} \right)^2 h_{1,k+1/2} h_{2,j+1/2} \sum_{i=1}^{n-2} x_{i+1}(1 - x_{i+1}) \tilde{h}_{1,i+1} \leq \\ &\leq \frac{1}{4} \sum_{j=0}^{n-1} \sum_{k=1}^{n-1} \left(\frac{u_{k+1,j} - u_{kj}}{h_{1,k+1/2}} \right)^2 h_{1,k+1/2} h_{2,j+1/2}. \end{aligned} \tag{3.27}$$

Performing an index shift and taking into account the homogeneous boundary condition $u_{i,0} = 0$ we get:

$$\begin{aligned} &\sum_{i=2}^{n-1} \sum_{j=1}^{n-1} u_{ij}^2 h_{2,j+1/2} \tilde{h}_{1,i} \leq \\ &\leq \frac{1}{4} \sum_{i=1}^{n-1} \sum_{j=0}^{n-1} \left(\frac{u_{i+1,j} - u_{ij}}{h_{1,i+1/2}} \right)^2 h_{1,i+1/2} h_{2,j+1/2}. \end{aligned} \tag{3.28}$$

Similar to (3.21) and (3.22), $u_{i,j+1}$ can be written in the following form, using that $u_{i,0} = u_{i,n} = 0$:

$$u_{i,j+1} = \sum_{k=0}^{j} \frac{u_{i,k+1} - u_{ik}}{\tilde{h}_{2,k+1}} \tilde{h}_{2,k+1}, \tag{3.29}$$

and

$$-u_{i,j+1} = \sum_{k=j+1}^{n-1} \frac{u_{i,k+1} - u_{ik}}{\tilde{h}_{2,k+1}} \tilde{h}_{2,k+1} \tag{3.30}$$

Performing similar steps as (3.23)-(3.28) and taking into account the homogeneous boundary condition $u_{1,j} = 0$ we get:

$$\begin{aligned} &\sum_{i=2}^{n-1} \sum_{j=1}^{n-1} u_{ij}^2 h_{2,j+1/2} \tilde{h}_{1,i} \leq \\ &\leq \frac{1}{4} \sum_{i=1}^{n-1} \sum_{j=0}^{n-1} \left(\frac{u_{i,j+1} - u_{ij}}{\tilde{h}_{2,j+1}} \right)^2 \tilde{h}_{1,i} \tilde{h}_{2,j+1}. \end{aligned} \tag{3.31}$$

Moreover for the v component:

$$\begin{aligned} &\sum_{i=1}^{n-1} \sum_{j=2}^{n-1} v_{ij}^2 h_{1,i+1/2} \tilde{h}_{2,j} \leq \\ &\leq \frac{1}{4} \sum_{i=0}^{n-1} \sum_{j=1}^{n-1} \left(\frac{v_{i+1,j} - v_{ij}}{\tilde{h}_{1,i+1}} \right)^2 \tilde{h}_{1,i+1} \tilde{h}_{2,j}. \end{aligned} \tag{3.32}$$

and

$$\begin{aligned} &\sum_{i=1}^{n-1} \sum_{j=2}^{n-1} v_{ij}^2 h_{1,i+1/2} \tilde{h}_{2,j} \leq \\ &\leq \frac{1}{4} \sum_{i=0}^{n-1} \sum_{j=1}^{n-1} \left(\frac{v_{i,j+1} - v_{ij}}{h_{2,j+1/2}} \right)^2 h_{2,j+1/2} h_{1,i+1/2}. \end{aligned} \tag{3.33}$$

Taking into account (3.28), (3.31), (3.32) and (3.33) and the definition of the norm $\|\vec{u}_h\|_{0,h^*}$, (3.18), and the scalar product $(A_{\underline{h}} \vec{u}_h, \vec{u}_h)_{0,h^*}$, (3.20), we get:

$$2\|\vec{u}_h\|_{0,h^*} \leq \frac{1}{4} (A_{\underline{h}} \vec{u}_h, \vec{u}_h)_{0,h^*},$$

that is

$$(A_{\underline{h}}\vec{u}_h, \vec{u}_h)_{0,h^*} = (D_{\underline{A}}A_{\underline{h}}\vec{u}_h, \vec{u}_h) \geq 8\|\vec{u}_h\|_{0,h^*} > 0,$$

if $\vec{u}_h \neq 0 \in \vec{V}_h \quad \bullet$.

Remark 1. The results of Theorem 1., Theorem 2. and Theorem 3. hold if Ω is a union of rectangles such that all the boundary lines of the different rectangles fit on the same global grid with grid spacing h_1 and h_2. $\bullet$

3.3 Numerical results

Below we show some computational results for the Stokes problem using the staggered grid approximation based on the finite volume method (3.14)-(3.17), (3.4), (3.6), on a non-equidistant grid in the unit square. Choosing different non-equidistant grid spacings we have maximized the rate of convergence for Uzawa-like methods, that is minimized $q_{Uz} := (\overline{\lambda_h} - \underline{\lambda_h})/(\overline{\lambda_h} + \underline{\lambda_h})$, where $\underline{\lambda_h}$ and $\overline{\lambda_h}$ are the smallest and the largest of the eigenvalues different from 0 and 1 of the discrete inf-sup problem, i.e. of $S_h = \tilde{B}_h A_{\underline{h}}^{-1} \tilde{B}_h^T$. (Then $[\underline{\lambda_h}, \overline{\lambda_h}]$ contains the eigenvalues corresponding to V_β and $\beta_h = \sqrt{\underline{\lambda_h}}$ is the discrete inf-sup constant.) We used the Matlab eig function to calculate the eigenvalues and the Matlab fmins function for minimization.

We found that the optimal grid is not an equidistant one, but a grid which is condensing in the center and coarser near the boundary of the unit square. Based on preliminary numerical experiments with arbitrary non-equidistant grids we chose a symmetrical grid with the same non-equidistant grid spacing in both directions.

That is we looked for a grid spacing in the following form:

$$\begin{aligned} h_{1,i-1/2} = h_{2,i-1/2} &= coef(0) - coef(1)i(1-i) - \\ &- coef(2)(i(1-i))^2 - coef(3)(i(1-i))^3, \end{aligned}$$

where $2 \le i \le \frac{n+1}{2}$ and we calculated the optimal grid spacing by changing the coefficients: $coef(k), 0 \le k \le 3$.

From the experimental results we found that there is no a real optimal grid, because the more condensed the grid is in the center, the smaller q_{Uz} is. For comparison bellow we gave a lower bound to the grid spacing in the center as follows: $h_{1,n/2} := \frac{1}{n-1}10^{-2}$ and optimized the grid with this restriction. In Table 1 we show the eigenvalues $\underline{\lambda_h}$ and $\overline{\lambda_h}$ related to this grid denoted by $\underline{\lambda_h}_{,*}$ and $\overline{\lambda_h}_{,*}$ in the case of $n = 11, 17, 23$. Because of the huge computational time for the grid optimization in the case of $n = 31, 51$ the optimal $\underline{\lambda_h}$ and $\overline{\lambda_h}$ were not calculated. In these cases $\underline{\lambda_h}_{,*}$ and $\overline{\lambda_h}_{,*}$ were calculated on a grid which is obtained by linearly interpolating the optimal grid for the case of $n = 23$.

We give also the smallest and the largest eigenvalues different from 0 and 1 in the case of an equidistant grid, denoted by $\underline{\lambda_h}_{,eq}$ and $\overline{\lambda_h}_{,eq}$, and in the practically used case when the grid is coarser in the center and condensing near the boundary of the unit square, denoted by $\underline{\lambda_h}_{,pr}$ and $\overline{\lambda_h}_{,pr}$. In this case we have determined the grid spacings by the following expression:

$$\begin{aligned} h_{1,i-1/2} &= 0.111737 - 0.006259i(1-i) - 0.000289(i(1-i))^2 - \\ &- 0.000011(i(1-i))^3, \end{aligned}$$

where $2 \leq i \leq \frac{n+1}{2}$. The grid here is symmetrical also with the same non-equidistant grid spacing in both directions. In the table, n denotes the number of grid points – including corner points – along a side of the square.

Table 1

n	11	17	23	31	51
$\underline{\lambda}_{h,*}$	0.6649	0.6647	0.6647	0.6646	0.6645
$\overline{\lambda}_{h,*}$	0.9999	0.9999	0.9999	0.9999	0.9999
$q_{*,Uz}$	0.2012	0.2014	0.2014	0.2015	0.2015
$q_{*,CG}$	0.1017	0.1017	0.1018	0.1018	0.1018
$\underline{\lambda}_{h,eq}$	0.4016	0.3489	0.3226	0.3022	0.2766
$\overline{\lambda}_{h,eq}$	0.8538	0.8545	0.8549	0.8552	0.8555
$q_{eq,Uz}$	0.3602	0.4202	0.4521	0.4778	0.5114
$q_{eq,CG}$	0.1864	0.2203	0.239	0.2544	0.275
$\underline{\lambda}_{h,pr}$	0.3507	0.2497	0.2168	0.2031	0.1933
$\overline{\lambda}_{h,pr}$	0.8429	0.8463	0.8469	0.847	0.847
$q_{pr,Uz}$	0.4124	0.5443	0.5923	0.6132	0.6284
$q_{pr,CG}$	0.2158	0.296	0.328	0.3426	0.3534

From these experimental results we can conclude that compared with the equidistant grid the use of such non-equidistant grids can economize between 58 and 140 percent of the computational work when iterating with an Uzawa-type method and between 36 and 78 percent for conjugate gradient-type methods, where

$$q_{CG} := (\sqrt{\overline{\lambda}_h} - \sqrt{\underline{\lambda}_h})/(\sqrt{\overline{\lambda}_h} + \sqrt{\underline{\lambda}_h}).$$

Compared with the practically used grid we can economize between 82 and 246 percent of the computational work for Uzawa-type methods and between 50 and 120 percent for conjugate gradient-type methods. Moreover, these numbers of gain in percent are increasing together with n. Finally, according to the table, the conjugate gradient-like methods are approximately one and a half times faster than the Uzawa-like ones, on the optimized grids.

4 Second order staggered grid approximation, non-standard and periodical boundary conditions

4.1 Second order staggered grid approximation

Now we consider the staggered grid approximation on an equidistant grid. For approximation of the Laplace operator with first order as usual for staggered grids, the grid has been supplemented by four lines at a distance $h/2$ from the boundary of the square, and fictitious zero values have been put into the u or v nodes on these lines, and then the standard five-point approximation of the Laplace operator has been used near the boundary as well. The supplementary values are needed also for the standard approximation of rot. To get a second order approximation, we do not need these supplementary four lines.

First we take the usual five-point approximation in the inner cells. The corresponding formulae can be obtained by simplifying (3.5) to our present case of an equidistant grid:

$$
\begin{aligned}
\Delta_{\overline{h}}\vec{u}_h &= (\Delta_{\overline{h}}u_h, \Delta_{\overline{h}}v_h)^T, \\
(\Delta_{\overline{h}}u_h)_{ij} &:= \frac{u_{i+1,j} - 2u_{ij} + u_{i-1,j}}{h^2} + \frac{u_{i,j+1} - 2u_{ij} + u_{i,j-1}}{h^2}, \\
& \quad\; 2 \le i \le n-1,\;\; 2 \le j \le n-2, \\
(\Delta_{\overline{h}}v_h)_{ij} &:= \frac{v_{i+1,j} - 2v_{ij} + v_{i-1,j}}{h^2} + \frac{v_{i,j+1} - 2v_{ij} + v_{i,j-1}}{h^2}, \\
& \quad\; 2 \le i \le n-2,\;\; 2 \le j \le n-1.
\end{aligned}
\tag{4.1}
$$

For the boundary cells, to get a second order approximation, we put now zero values into additional u or v nodes on the original boundary. These additional points are at a distance of $h/2$ from the nearest u or v point. Therefore, the approximation in the boundary cells will be different from that in the inner cells:

$$
\begin{aligned}
(\Delta_{\overline{h}} u_h)_{i,1} &:= \frac{u_{i+1,1} - 2u_{i,1} + u_{i-1,1}}{h^2} + \frac{1}{h}\left(\frac{u_{i,2} - u_{i,1}}{h} - \frac{u_{i,1} - u_{i,0}}{h/2}\right), \\
(\Delta_{\overline{h}} u_h)_{i,n-1} &:= \frac{u_{i+1,n-1} - 2u_{i,n-1} + u_{i-1,n-1}}{h^2} + \\
&\quad + \frac{1}{h}\left(\frac{u_{i,n} - u_{i,n-1}}{h/2} - \frac{u_{i,n-1} - u_{i,n-2}}{h}\right), \quad 2 \le i \le n-1, \\
(\Delta_{\overline{h}} v_h)_{1,j} &:= \frac{1}{h}\left(\frac{v_{2,j} - v_{1,j}}{h} - \frac{v_{1,j} - v_{0,j}}{h/2}\right) + \frac{v_{1,j+1} - 2v_{1,j} + v_{1,j-1}}{h^2}, \\
(\Delta_{\overline{h}} v_h)_{n-1,j} &:= \frac{1}{h}\left(\frac{v_{n,j} - v_{n-1,j}}{h/2} - \frac{v_{n-1,j} - v_{n-2,j}}{h}\right) + \\
&\quad + \frac{v_{n-1,j+1} - 2v_{n-1,j} + v_{n-1,j-1}}{h^2}, \quad 2 \le j \le n-1.
\end{aligned}
$$

Here $u_{i,0}, u_{i,n}, v_{0,j}, v_{n,j}$ are the additional zero values on the boundary. The discrete divergence is the same as in (3.4):

$$
(\mathrm{div}_{\overline{h}}\, \vec{u}_h)_{ij} := \frac{u_{i+1,j} - u_{ij}}{h} + \frac{v_{i,j+1} - v_{ij}}{h}, \qquad 1 \le i, j \le n-1,
$$

and the discrete rotation is:

$$
\begin{aligned}
(\mathrm{rot}_{\overline{h}}\, \vec{u}_h)_{ij} &:= \frac{v_{i+1,j} - v_{ij}}{h} - \frac{u_{i+1,j} - u_{i+1,j-1}}{h}, \\
&\quad 1 \le i \le n-2, \ 2 \le j \le n-1, \\
(\mathrm{rot}_{\overline{h}}\, \vec{u}_h)_{i,1} &:= \frac{v_{i+1,1} - v_{i,1}}{h} - \frac{u_{i+1,1} - u_{i+1,0}}{h/2}, \\
(\mathrm{rot}_{\overline{h}}\, \vec{u}_h)_{i,n} &:= \frac{v_{i+1,n} - v_{i,n}}{h} - \frac{u_{i+1,n} - u_{i+1,n-1}}{h/2}, \\
&\quad 1 \le i \le n-2, \\
(\mathrm{rot}_{\overline{h}}\, \vec{u}_h)_{0,j} &:= \frac{v_{1,j} - v_{0,j}}{h/2} - \frac{u_{1,j} - u_{1,j-1}}{h}, \\
(\mathrm{rot}_{\overline{h}}\, \vec{u}_h)_{n-1,j} &:= \frac{v_{n,j} - v_{n-1,j}}{h/2} - \frac{u_{n,j} - u_{n,j-1}}{h}, \\
&\quad 2 \le j \le n-1,
\end{aligned}
\tag{4.2}
$$

The discrete L_2 scalar products (3.1) and (3.3) simplify to

$$
(p_h, q_h)_{0,h} := \sum_{i,j=1}^{n-1} p_{ij} q_{ij} h^2, \tag{4.3}
$$

$$
(\vec{u}_h, \vec{w}_h)_{0,h} := \sum_{i=2}^{n-1} \sum_{j=1}^{n-1} u_{ij} r_{ij} h^2 + \sum_{i=1}^{n-1} \sum_{j=2}^{n-1} v_{ij} s_{ij} h^2, \tag{4.4}
$$

where p_h, q_h are pressure vectors and $\vec{u}_h = (u_h, v_h)^T$, $\vec{w}_h = (r_h, s_h)^T$ are velocity vectors.

$$\|p_h\|_{0,h}^2 := (p_h, p_h)_{0,h}, \quad \|\vec{u}_h\|_{0,h}^2 := (\vec{u}_h, \vec{u}_h)_{0,h}.$$

Theorem 4. For the second order staggered grid approximation,

$$\begin{aligned}(A_{\overline{h}}\vec{u}_h, \vec{u}_h)_{0,h} &- \|\tilde{B}_{\overline{h}}\vec{u}_h\|_{0,h}^2 - \|\tilde{C}_{\overline{h}}\vec{u}_h\|_{0,h}^2 = \\ &= -\sum_{i=2}^{n-1} 2(u_{i,1}^2 + u_{i,n-1}^2) - \sum_{j=2}^{n-1} 2(v_{1,j}^2 + v_{n-1,j}^2), \quad (4.5)\end{aligned}$$

where $\tilde{B}_{\overline{h}} := -div_{\overline{h}}$ and $\tilde{C}_{\overline{h}} := rot_{\overline{h}}$.

Proof. Similarly to the proof of Theorem 1 we apply partial summation to $(A_{\overline{h}}\vec{u}_h, \vec{u}_h)_{0,h}$ and then continue the grid functions u_h and v_h by zero onto the grid of the whole two-dimensional plane. Taking into account that

$$u_{i,0}, u_{i,n}, v_{0,j}, v_{n,j}, u_{1,j}, u_{n,j}, v_{i,1}, v_{i,n}$$

are zero if $1 \le i, j \le n-1$, we may write:

$$\begin{aligned}(A_{\overline{h}}\vec{u}_h, \vec{u}_h)_{0,h} &= \sum_{i,j} \Big((u_{i+1,j} - u_{ij})^2 + (u_{i,j+1} - u_{ij})^2 + \\ &\quad + (v_{i+1,j} - v_{ij})^2 + (v_{i,j+1} - v_{ij})^2 \Big) + \\ &\quad + \sum_{i=2}^{n-1}(u_{i,1}^2 + u_{i,n-1}^2) + \sum_{j=2}^{n-1}(v_{1,j}^2 + v_{n-1,j}^2), \\ \|\tilde{B}_{\overline{h}}\vec{u}_h\|_{0,h}^2 &= \sum_{i,j} \Big((u_{i+1,j} - u_{ij})^2 + (v_{i,j+1} - v_{ij})^2 + \\ &\quad + 2(u_{i+1,j} - u_{ij})(v_{i,j+1} - v_{ij}) \Big), \\ \|\tilde{C}_{\overline{h}}\vec{u}_h\|_{0,h}^2 &= \sum_{i,j} \Big((u_{i+1,j} - u_{i+1,j-1})^2 + (v_{i+1,j} - v_{ij})^2 - \\ &\quad - 2(u_{i+1,j} - u_{i+1,j-1})(v_{i+1,j} - v_{ij}) \Big) + \\ &\quad + \sum_{i=1}^{n-2}(3u_{i+1,1}^2 + 3u_{i+1,n-1}^2) + \sum_{j=2}^{n-1}(3v_{1,j}^2 + 3v_{n-1,j}^2),\end{aligned}$$

Performing the same index shifts as during the proof of Theorem 1, we get the result of Theorem 3. $\bullet$

Remark 1. We introduce the notation $\tilde{A}_{\overline{h}}$, where

$$(\tilde{A}_{\overline{h}}\vec{u}_h, \vec{u}_h)_{0,h} = (A_{\overline{h}}\vec{u}_h, \vec{u}_h)_{0,h} + \sum_{i=2}^{n-1} 2(u_{i,1}^2 + u_{i,n-1}^2) + \sum_{j=2}^{n-1} 2(v_{1,j}^2 + v_{n-1,j}^2).$$

$\tilde{A}_{\overline{h}}$ is a symmetric positive definite matrix in the sense of (4.4), together with $A_{\overline{h}}$. Since $\dim(V_{h0}) = (n-2)^2$, $\dim(V_{h1}) = (n-3)^2$ and $\dim(V_{h,\beta}) = 4n-9$, a proper Crouzeix–Velte decomposition exists in this case as well, for $n > 3$. In this case the algebraic decomposition exists not for the matrix $A_{\overline{h}}$,but for $\tilde{A}_{\overline{h}}$, hence $\tilde{A}_{\overline{h}}$ can be advantageous as a preconditional matrix solving $A_{\overline{h}}\vec{u}_h = b_h$. Let us mention that in [8] there appears an analytical counterpart of (4.5). •

4.2 Non-standard boundary conditions

The following Theorem is proved in [25]:

Theorem 5. Let Ω be a two-dimensional domain with Lipschitz – continuous, piecewise C^2 boundary Γ satisfying $1/r \in L_\infty(\Gamma)$ where $r(s)$ is the curvature in $s \in \Gamma$. Then a Crouzeix-Velte decomposition exists in the analytical case if, for the Laplace operator $A = -\Delta$, either of the following two boundary conditions are prescribed on Γ:

$$\vec{u} \cdot \vec{n} = 0 \text{ and } \operatorname{rot} \vec{u} = 0; \tag{4.6}$$

or

$$\vec{u} \times \vec{n} = 0 \text{ and } \operatorname{div} \vec{u} = 0. \quad \bullet \tag{4.7}$$

The boundary conditions (4.6), (4.7) may be unusual, but they satisfy the Lopatinski-condition (see [20] or [3], there the complementing condition), as can be verified straightforwardly for both $d = 2$ and $d = 3$ (where (4.6) takes the form $\operatorname{rot} \vec{u} \times \vec{n} = 0$). Condition (4.6) appears, e.g. also in [4] and allows to calculate the pressure independent of $\vec{u}$.

Now we consider the discrete equivalent of Theorem 5. In addition to (4.3) and (4.4) we introduce the following discrete scalar product and the corresponding norm:

$$\begin{aligned} (p_h, q_h)_{0,\tilde{h}} &:= \sum_{i=1}^{n-2} \sum_{j=2}^{n-1} p_{ij} q_{ij} h^2, \\ \|p_h\|^2_{0,\tilde{h}} &:= (p_h, p_h)_{0,\tilde{h}}. \end{aligned} \tag{4.8}$$

The divergence is approximated as usual:

$$(\operatorname{div}_h \vec{u}_h)_{ij} := \frac{u_{i+1,j} - u_{ij}}{h} + \frac{v_{i,j+1} - v_{ij}}{h}, \tag{4.9}$$

where $1 \le i, j \le n-1$, $\vec{u}_h := (u_h, v_h)^T$. We approximate the Laplace operator with first order, and the rotation in the corner points of inner cells as follows:

$$(\operatorname{rot}_h \vec{u}_h)_{ij} := \frac{v_{i+1,j} - v_{ij}}{h} - \frac{u_{i+1,j} - u_{i+1,j-1}}{h}, \tag{4.10}$$

where $1 \le i \le n-2, \ 2 \le j \le n-1$.

We consider now the following nonstandard boundary conditions, which are the discrete equivalent of (4.6):

$$u_{1,j} = u_{n,j} = v_{i,1} = v_{i,n} = 0, \tag{4.11}$$

for $1 \leq i \leq n-1,\ \ 1 \leq j \leq n-1$, and

$$(\mathrm{rot}_h\, \vec{u}_h)_{0,j} = (\mathrm{rot}_h\, \vec{u}_h)_{n-1,j} = (\mathrm{rot}_h\, \vec{u}_h)_{i,1} = (\mathrm{rot}_h\, \vec{u}_h)_{i,n} = 0, \tag{4.12}$$

for $0 \leq i \leq n-1,\ \ 2 \leq j \leq n-1$, where rot_h is defined similarly to (4.10), using also the additional grid-lines. Finally, now for our specific difference discretization, we continue to use the notations A_h, $\tilde{B}_h$, and $\tilde{C}_h$ for the matrices of the operators $-\Delta_h$, $-\mathrm{div}_h$ and rot_h, respectively.

Theorem 6. For the staggered grid approximation (4.9), (4.10) and the standard five-point approximation of the Laplace-operator with boundary conditions (4.11) and (4.12) the following relation holds:

$$(A_h\vec{u}_h, \vec{u}_h)_{0,h} = \|\tilde{B}_h\vec{u}_h\|^2_{0,h} + \|\tilde{C}_h\vec{u}_h\|^2_{0,\tilde{h}}$$

for all vectors $\vec{u}_h = (u_h, v_h)^T$.

Proof. Applying partial summation to $(A_h\vec{u}_h, \vec{u}_h)_{0,h}$ we obtain:

$$\begin{aligned}
(A_h\vec{u}_h, \vec{u}_h)_{0,h} &= \sum_{i=2}^{n-2}\sum_{j=1}^{n-1}(u_{i+1,j} - u_{ij})^2 + \sum_{j=1}^{n-1}(u_{2,j} - u_{1,j})u_{2,j} - \\
&- \sum_{j=1}^{n-1}(u_{n,j} - u_{n-1,j})u_{n-1,j} + \sum_{i=2}^{n-1}\sum_{j=1}^{n-2}(u_{i,j+1} - u_{ij})^2 + \\
&+ \sum_{i=2}^{n-1}(u_{i,1} - u_{i,0})u_{i,1} - \sum_{i=2}^{n-1}(u_{i,n} - u_{i,n-1})u_{i,n-1} + \\
&+ \sum_{i=1}^{n-2}\sum_{j=2}^{n-1}(v_{i+1,j} - v_{ij})^2 + \sum_{j=2}^{n-1}(v_{1,j} - v_{0,j})v_{1,j} - \\
&- \sum_{j=2}^{n-1}(v_{n,j} - v_{n-1,j})v_{n-1,j} + \sum_{i=1}^{n-1}\sum_{j=2}^{n-2}(v_{i,j+1} - v_{ij})^2 + \\
&+ \sum_{i=1}^{n-1}(v_{i,2} - v_{i,1})v_{i,2} - \sum_{i=1}^{n-1}(v_{i,n} - v_{i,n-1})v_{i,n-1}.
\end{aligned}$$

Using the boundary conditions (4.11) and (4.12), we find:

$$
\begin{aligned}
(A_h\vec{u}_h, \vec{u}_h)_{0,h} &= \sum_{i=2}^{n-2}\sum_{j=1}^{n-1}(u_{i+1,j}-u_{ij})^2 + \sum_{i=2}^{n-1}\sum_{j=1}^{n-2}(u_{i,j+1}-u_{ij})^2 + \\
&+ \sum_{i=1}^{n-2}\sum_{j=2}^{n-1}(v_{i+1,j}-v_{ij})^2 + \sum_{i=1}^{n-1}\sum_{j=2}^{n-2}(v_{i,j+1}-v_{ij})^2 + \\
&+ \sum_{j=1}^{n-1}u_{2,j}^2 + \sum_{j=1}^{n-1}u_{n-1,j}^2 + \sum_{i=1}^{n-1}v_{i,2}^2 + \sum_{i=1}^{n-1}v_{i,n-1}^2. \qquad (4.13)
\end{aligned}
$$

Further, $\|\tilde{B}_h\vec{u}_h\|_{0,h}^2$ may be written as follows:

$$
\begin{aligned}
\|\tilde{B}_h\vec{u}_h\|_{0,h}^2 &= \sum_{i,j=1}^{n-1}(u_{i+1,j}-u_{ij})^2 + \sum_{i,j=1}^{n-1}(v_{i,j+1}-v_{ij})^2 + \\
&+ 2\sum_{i,j=1}^{n-1}(u_{i+1,j}-u_{ij})(v_{i,j+1}-v_{ij}) = \qquad (4.14) \\
&= \sum_{i=2}^{n-2}\sum_{j=1}^{n-1}(u_{i+1,j}-u_{ij})^2 + \sum_{i=1}^{n-1}\sum_{j=2}^{n-2}(v_{i,j+1}-v_{ij})^2 + \\
&+ \sum_{j=1}^{n-1}u_{2,j}^2 + \sum_{j=1}^{n-1}u_{n-1,j}^2 + \sum_{i=1}^{n-1}v_{i,2}^2 + \sum_{i=1}^{n-1}v_{i,n-1}^2 + \\
&+ 2\sum_{i,j=1}^{n-1}(u_{i+1,j}-u_{ij})(v_{i,j+1}-v_{ij}).
\end{aligned}
$$

Using the boundary conditions, the discrete rotation is calculated only in the corners of inner cells, and $\|\tilde{C}_h\vec{u}_h\|_{0,\tilde{h}}^2$ can be written as follows:

$$
\begin{aligned}
\|\tilde{C}_h\vec{u}_h\|_{0,\tilde{h}}^2 &= \sum_{i=1}^{n-2}\sum_{j=2}^{n-1}(u_{i+1,j}-u_{i+1,j-1})^2 + \sum_{i=1}^{n-2}\sum_{j=2}^{n-1}(v_{i+1,j}-v_{ij})^2 - \\
&- 2\sum_{i=1}^{n-2}\sum_{j=2}^{n-1}(u_{i+1,j}-u_{i+1,j-1})(v_{i+1,j}-v_{ij}) = \qquad (4.15) \\
&= \sum_{i=2}^{n-1}\sum_{j=1}^{n-2}(u_{i,j+1}-u_{i,j})^2 + \sum_{i=1}^{n-2}\sum_{j=2}^{n-1}(v_{i+1,j}-v_{ij})^2 - \\
&- 2\sum_{i=1}^{n-2}\sum_{j=2}^{n-1}(u_{i+1,j}-u_{i+1,j-1})(v_{i+1,j}-v_{ij}).
\end{aligned}
$$

Performing some index shifts we obtain from the last term in (4.14):

$$2\sum_{i,j=1}^{n-1}(u_{i+1,j} - u_{ij})(v_{i,j+1} - v_{ij}) = 2\sum_{i=1}^{n-1}\sum_{j=2}^{n} u_{i+1,j-1}v_{ij} - 2\sum_{i,j=1}^{n-1} u_{i+1,j}v_{ij} -$$
$$- \quad 2\sum_{i=0}^{n-2}\sum_{j=2}^{n} u_{i+1,j-1}v_{i+1,j} + 2\sum_{i=0}^{n-2}\sum_{j=1}^{n-1} u_{i+1,j}v_{i+1,j}. \qquad (4.16)$$

Performing some further index shifts and using the boundary condition (4.11), from (4.16), and including the last term of (4.15), we find:

$$2\sum_{i,j=1}^{n-1}(u_{i+1,j} - u_{ij})(v_{i,j+1} - v_{ij}) - 2\sum_{i=1}^{n-2}\sum_{j=2}^{n-1}(u_{i+1,j} - u_{i+1,j-1})(v_{i+1,j} - v_{ij}) =$$
$$= \quad 2\sum_{j=1}^{n-1} u_{1,j}(v_{1,j} - v_{1,j+1}) + 2\sum_{j=1}^{n-1} u_{n,j}(v_{n-1,j+1} - v_{n-1,j}) + \qquad (4.17)$$
$$+ \quad 2\sum_{i=1}^{n-1} v_{i,n}(u_{i+1,n-1} - u_{i,n-1}) + 2\sum_{i=1}^{n-1} v_{i,1}(u_{i,1} - u_{i+1,1}) = 0.$$

From (4.13) – (4.17) we get:

$$(A_h\vec{u}_h, \vec{u}_h)_{0,h} - \|\tilde{B}_h\vec{u}_h\|^2_{0,h} - \|\tilde{C}_h\vec{u}_h\|^2_{0,\tilde{h}} = 0. \quad \bullet$$

Remark 1. Taking into account the boundary conditions (4.11) and (4.12), the number n_h of velocity degrees of freedom is $n_h := 2(n-2)(n-1) + 4(n-2)$.

It can be shown that $\dim(V_{h,0}) := \dim\ker\operatorname{div}_h = (n-2)^2$. Namely, to compute this dimension we count the number of conditions to get $\|\operatorname{div}_h\vec{u}_h\|^2_{0,h} = 0$. Excluding the very last cell (which is depending on the other cells) we have to require $\operatorname{div}_h\vec{u}_h = 0$ in all remaining cells, that is, in $(n-1)^2 - 1$ points. In addition to it we have to require $\operatorname{rot}_h\vec{u}_h = 0$ in the cell corners on the boundary, that is, in $4(n-2)$ points, because of the boundary condition (4.12). Then $\dim\ker\operatorname{div}_h = n_h - ((n-1)^2 - 1) - 4(n-2) = (n-2)^2$. Similarly, to compute $\dim(V_{h,1}) = \dim\ker\operatorname{rot}_h$ we count the number of conditions to get $\|\operatorname{rot}_h\vec{u}_h\|^2_{0,h} = 0$, starting from the boundary of the grid and proceeding to the center. Excluding the corners of the square, in all other cell corners we have to require $\operatorname{rot}_h\vec{u}_h = 0$, that is in $n^2 - 4$ points. Then $\dim\ker\operatorname{rot}_h = n_h - (n^2 - 4) = n^2 - 2n$. Therefore, $\dim(V_{h,\beta}) = n_h - (n-2)^2 - (n^2 - 2n) = 4n - 8 > 0$, if $n \geq 3$. Since A_h is a symmetric positive definite matrix in the sense of the scalar product (4.4), a proper Crouzeix-Velte decomposition exists. (For the proof, see Remark 3. in the following subsection.) •

Remark 2. To obtain a second order approximation for the boundary cells, too, we put values not into the supplementary lines but into additional u or v nodes on the original boundary. It can be shown that the discrete Crouzeix-Velte decomposition exists in this case for the matrix A_h as well, in contrast to the case of Dirichlet boundary conditions, where we proved the existence of the decomposition only for $\widetilde{A}_{\overline{h}}$, see: Remark 1. in the previous subsection. •

Remark 3. Considering the discrete equivalent of the boundary conditions (4.7), it can be shown similarly to Theorem 6, that a discrete Crouzeix-Velte decomposition exists for both the first and second order approximation. •

4.3 Periodical boundary conditions

As we show in this point, the results of [21] on the existence of a Crouzeix-Velte decomposition for the Stokes problem along with Dirichlet and periodical boundary conditions carry over to the discrete case for the staggered grid approximation.

For the first order approximation we use the same grid as used in the previous subsection. Periodical boundary conditions are assumed on the left and right sides of the unit square:

$$\begin{aligned} u_{1,j} = u_{n-1,j}, u_{2,j} = u_{n,j}, &\quad 0 \leq j \leq n, \\ v_{1,j} = v_{n-1,j}, v_{2,j} = v_{n,j}, &\quad 1 \leq j \leq n. \end{aligned} \tag{4.18}$$

On the upper and lower sides of the unit square we prescribe homogeneous Dirichlet conditions:

$$\begin{aligned} u_{i,0} = u_{i,n} = 0, &\quad 1 \leq i \leq n, \\ v_{i,1} = v_{i,n} = 0, &\quad 1 \leq i \leq n-1, \end{aligned} \tag{4.19}$$

where $u_{i,0}, u_{i,n}$ are values on two additional grid lines, which the grid has been supplemented with. The approximation of the divergence, Laplace operator and the rotation are the same as in the previous subsection, but we have to take into account the periodical boundary conditions on the left and right boundaries of the unit square. The divergence is, once more, approximated by (4.9), but now for $1 \leq i \leq n-2, 1 \leq j \leq n-1$. The approximation of the Laplace operator with first order is:

$$\begin{aligned} \Delta_h \vec{u}_h &= (\Delta_h u_h, \Delta_h v_h)^T, \\ (\Delta_h u_h)_{ij} &:= \frac{u_{i+1,j} - 2u_{ij} + u_{i-1,j}}{h^2} + \frac{u_{i,j+1} - 2u_{ij} + u_{i,j-1}}{h^2}, \\ & \quad\; 2 \leq i \leq n-1,\ 1 \leq j \leq n-1, \\ (\Delta_h v_h)_{ij} &:= \frac{v_{i+1,j} - 2v_{ij} + v_{i-1,j}}{h^2} + \frac{v_{i,j+1} - 2v_{ij} + v_{i,j-1}}{h^2}, \\ & \quad\; 2 \leq i \leq n-1,\ 2 \leq j \leq n-1. \end{aligned}$$

Finally, the approximation of the rotation is given by (4.10) as earlier but now for $1 \leq i \leq n-2,\ 1 \leq j \leq n$. Instead of (4.3) and (4.4) and (4.8) we introduce the discrete scalar products and corresponding norms as follows:

$$
\begin{aligned}
(p_h, q_h)_{0,h} &:= \sum_{i=1}^{n-2}\sum_{j=1}^{n-1} p_{ij}q_{ij}h^2, \\
(p_h, q_h)_{0,\tilde{h}} &:= \sum_{i=1}^{n-2}\sum_{j=1}^{n} p_{ij}q_{ij}h^2, \\
(\vec{u}_h, \vec{w}_h)_{0,h} &:= \sum_{i=2}^{n-1}\sum_{j=1}^{n-1} u_{ij}r_{ij}h^2 + \sum_{i=2}^{n-1}\sum_{j=2}^{n-1} v_{ij}s_{ij}h^2,
\end{aligned}
$$

$$
\|p_h\|^2_{0,h} := (p_h, p_h)_{0,h}, \quad \|p_h\|^2_{0,\tilde{h}} := (p_h, p_h)_{0,\tilde{h}}, \quad \|\vec{u}_h\|^2_{0,h} := (\vec{u}_h, \vec{u}_h)_{0,h}.
$$

Once again, A_h, $\tilde{B}_h$, and $\tilde{C}_h$ denote the matrices of the operators $-\Delta_h$, $-\operatorname{div}_h$ and rot_h.

Theorem 7.

$$
(A_h\vec{u}_h, \vec{u}_h)_{0,h} = \|\tilde{B}_h\vec{u}_h\|^2_{0,h} + \|\tilde{C}_h\vec{u}_h\|^2_{0,\tilde{h}}
$$

holds for all vectors $\vec{u}_h = (u_h, v_h)^T$ satisfying the boundary conditions (4.18) and (4.19).

Proof. The proof is similar to that of Theorem 6. We apply partial summation to $(A_h\vec{u}_h, \vec{u}_h)_{0,h}$, and taking into account the boundary conditions we obtain:

$$
\begin{aligned}
(A_h\vec{u}_h, \vec{u}_h)_{0,h} &= \sum_{i=1}^{n-2}\sum_{j=1}^{n-1}(u_{i+1,j} - u_{ij})^2 + \sum_{i=2}^{n-1}\sum_{j=1}^{n-2}(u_{i,j+1} - u_{ij})^2 + \\
&+ \sum_{i=1}^{n-2}\sum_{j=2}^{n-1}(v_{i+1,j} - v_{ij})^2 + \sum_{i=1}^{n-2}\sum_{j=2}^{n-2}(v_{i,j+1} - v_{ij})^2 + \\
&+ \sum_{i=2}^{n-1} u^2_{i,n-1} + \sum_{i=2}^{n-1} u^2_{i,1} + \sum_{i=1}^{n-2} v^2_{i,2} + \sum_{i=1}^{n-2} v^2_{i,n-1}. \qquad (4.20)
\end{aligned}
$$

$\|\tilde{B}_h\vec{u}_h\|^2_{0,h}$ can be written as follows:

$$
\begin{aligned}
\|\tilde{B}_h\vec{u}_h\|^2_{0,h} &= \sum_{i=1}^{n-2}\sum_{j=1}^{n-1}(u_{i+1,j} - u_{ij})^2 + \sum_{i=1}^{n-2}\sum_{j=1}^{n-1}(v_{i,j+1} - v_{ij})^2 + \\
&+ 2\sum_{i=1}^{n-2}\sum_{j=1}^{n-1}(u_{i+1,j} - u_{ij})(v_{i,j+1} - v_{ij}). \qquad (4.21)
\end{aligned}
$$

$\|\tilde{C}_h\vec{u}_h\|^2_{0,\tilde{h}}$ can be simplified (taking account of the homogeneous Dirichlet conditions) to the following form:

$$
\begin{aligned}
\|\tilde{C}_h\vec{u}_h\|^2_{0,\tilde{h}} &= \sum_{i=1}^{n-2}\sum_{j=1}^{n}(u_{i+1,j}-u_{i+1,j-1})^2+\sum_{i=1}^{n-2}\sum_{j=1}^{n}(v_{i+1,j}-v_{ij})^2 - \\
&- 2\sum_{i=1}^{n-2}\sum_{j=1}^{n}(u_{i+1,j}-u_{i+1,j-1})(v_{i+1,j}-v_{ij}) = \\
&= \sum_{i=1}^{n-2}\sum_{j=2}^{n-1}(u_{i+1,j}-u_{i+1,j-1})^2+\sum_{i=1}^{n-2}\sum_{j=2}^{n-1}(v_{i+1,j}-v_{ij})^2 - \\
&- 2\sum_{i=1}^{n-2}\sum_{j=2}^{n-1}(u_{i+1,j}-u_{i+1,j-1})(v_{i+1,j}-v_{ij}) + \\
&+ \sum_{i=1}^{n-2}u^2_{i+1,1}+\sum_{i=1}^{n-2}u^2_{i+1,n-1}.
\end{aligned}
\tag{4.22}
$$

Performing some index shifts and using the boundary conditions (4.18) and (4.19), we find for the sum of the expressions standing in lines (4.21) and (4.22):

$$
\begin{aligned}
&-2\sum_{i=1}^{n-2}\sum_{j=1}^{n-1}(u_{i+1,j}-u_{ij})(v_{i,j+1}-v_{ij}) + \\
&\quad + 2\sum_{i=1}^{n-2}\sum_{j=2}^{n-1}(u_{i+1,j}-u_{i+1,j-1})(v_{i+1,j}-v_{ij})) = \\
&\quad = -2\sum_{i=1}^{n-2}u_{i+1,n-1}v_{i,n}-2\sum_{i=1}^{n-2}u_{i+1,1}v_{i,1}+2\sum_{j=1}^{n-2}u_{n-1,j}v_{n-1,j+1} - \\
&\quad - 2\sum_{i=1}^{n-2}u_{i,n-1}v_{i,n}-2\sum_{j=1}^{n-2}u_{1,j}v_{1,j+1}+2\sum_{j=2}^{n-1}u_{n-1,j}v_{n-1,j} - \\
&\quad - 2\sum_{j=2}^{n-1}u_{1,j}v_{1,j}-2\sum_{i=1}^{n-2}u_{i,1}v_{i,1}=0.
\end{aligned}
\tag{4.23}
$$

From (4.20) - (4.23) – performing some index shifts and using the homogeneous Dirichlet boundary conditions – we obtain:

$$(A_h\vec{u}_h,\vec{u}_h)_{0,h} - \|\tilde{B}_h\vec{u}_h\|^2_{0,h} - \|\tilde{C}_h\vec{u}_h\|^2_{0,\tilde{h}} =$$
$$= \sum_{i=1}^{n-2} v_{i,2}^2 + \sum_{i=1}^{n-2} v_{i,n-1}^2 - \sum_{i=1}^{n-2}(v_{i,2}-v_{i,1})^2 - \sum_{i=1}^{n-2}(v_{i,n}-v_{i,n-1})^2 = 0.$$

•

Remark 1. Taking into account the boundary conditions (4.18) and (4.19), it can be shown that the number of velocity degrees of freedom is $n_h := (n-2)(n-1)+(n-2)^2$, $\dim(V_{h,0}) := \dim\ker\operatorname{div}_h = (n-2)^2+1$ and $\dim(V_{h,1}) := \dim\ker\operatorname{rot}_h = n^2-5n+7$. Therefore $\dim(V_{h,\beta}) = n_h - ((n-2)^2+1) - (n^2-5n+7) = 2n-6 > 0$ if $n > 3$. •

Remark 2. A_h is a positive definite matrix.

Proof.

Taking into account (4.20) and the boundary conditions we obtain:

$$\begin{aligned}
(A_h\vec{u}_h,\vec{u}_h)_{0,h} &\geq \sum_{i=2}^{n-1}\sum_{j=1}^{n-2}(u_{i,j+1}-u_{ij})^2 + \sum_{i=1}^{n-2}\sum_{j=2}^{n-2}(v_{i,j+1}-v_{ij})^2 + \\
&+ \sum_{i=2}^{n-1} u_{i,n-1}^2 + \sum_{i=2}^{n-1} u_{i,1}^2 + \sum_{i=1}^{n-2} v_{i,2}^2 + \sum_{i=1}^{n-2} v_{i,n-1}^2 = \\
&= \sum_{i=2}^{n-1}\sum_{j=0}^{n-1}(u_{i,j+1}-u_{ij})^2 + \sum_{i=1}^{n-2}\sum_{j=1}^{n-1}(v_{i,j+1}-v_{ij})^2
\end{aligned} \tag{4.24}$$

Here $u_{i,j+1}$ also can be written in the following form, using that $u_{i,0} = u_{i,n} = 0$:

$$u_{i,j+1} = \sum_{k=0}^{j} \frac{u_{i,k+1}-u_{ik}}{h} h, \tag{4.25}$$

and

$$-u_{i,j+1} = \sum_{k=j+1}^{n-1} \frac{u_{i,k+1}-u_{ik}}{h} h \tag{4.26}$$

Using the Cauchy inequality, similarly to the steps (3.23) - (3.28) it follows:

$$u_{i,j+1}^2 \leq (1-y_i)y_i \sum_{k=0}^{n-1} \left(\frac{u_{i,k+1}-u_{ik}}{h}\right)^2 h, \tag{4.27}$$

Multiplying by h and summarizing according to i:

$$\sum_{i=2}^{n-1} u_{i,j+1}^2 h \leq \tag{4.28}$$
$$(1-y_i)y_i \sum_{i=2}^{n-1}\sum_{k=0}^{n-1}\left(\frac{u_{i,k+1}-u_{ik}}{h}\right)^2 h^2,$$

and finally

$$\sum_{i=2}^{n-1}\sum_{j=0}^{n-1} u_{i,j+1}^2 h^2 \leq \tag{4.29}$$
$$\leq \sum_{i=2}^{n-1}\sum_{k=0}^{n-1}\left(\frac{u_{i,k+1}-u_{ik}}{h}\right)^2 h^2 \sum_{j=0}^{n-1}(1-y_i)y_i h.$$

Performing an index shift and taking into account that $u_{in}=0$ and

$$\sum_{j=0}^{n-1}(1-y_i)y_i h = \sum_{j=0}^{n-1}(n-i)ih^3 = h^3 n(n-1)\left(\frac{n}{2}-\frac{2n-1}{6}\right) = \frac{1-h^2}{6} < \frac{1}{6},$$

we obtain:

$$\sum_{i=2}^{n-1}\sum_{j=1}^{n-1} u_{i,j}^2 h^2 \leq \tag{4.30}$$
$$\leq \frac{1}{6}\sum_{i=2}^{n-1}\sum_{j=0}^{n-1}\left(u_{i,j+1}-u_{ij}\right)^2.$$

We can also obtain:

$$\sum_{i=2}^{n-1}\sum_{j=2}^{n-1} v_{i,j}^2 h^2 \leq \tag{4.31}$$
$$\leq \frac{1}{6}\sum_{i=1}^{n-2}\sum_{j=1}^{n-1}\left(v_{i,j+1}-v_{ij}\right)^2.$$

That is from (4.24), (4.30) and (4.31):

$$(A_h\vec{u}_h,\vec{u}_h)_{0,h} \geq 6\|\vec{u}_h\|_{0,h}^2 > 0$$
$$\text{if } \vec{u}_h \neq 0 \in \vec{V}_h. \quad \bullet$$

Remark 3.

A_h is a positive definit matrix in the case of non-standard boundary conditions, as well. In this case, using the boundary conditions (4.11) and (4.12), we find:

$$\begin{aligned}(A_h\vec{u}_h, \vec{u}_h)_{0,h} &= \sum_{i=1}^{n-1}\sum_{j=1}^{n-1}(u_{i+1,j} - u_{ij})^2 + \sum_{i=2}^{n-1}\sum_{j=1}^{n-2}(u_{i,j+1} - u_{ij})^2 + \\ &+ \sum_{i=1}^{n-2}\sum_{j=2}^{n-1}(v_{i+1,j} - v_{ij})^2 + \sum_{i=1}^{n-1}\sum_{j=1}^{n-1}(v_{i,j+1} - v_{ij})^2 \geq \\ &\geq \sum_{i=1}^{n-1}\sum_{j=1}^{n-1}(u_{i+1,j} - u_{ij})^2 + \sum_{i=1}^{n-1}\sum_{j=1}^{n-1}(v_{i,j+1} - v_{ij})^2.\end{aligned}$$

Using similar steps as in the case of periodical boundary conditions we obtain:

$$(A_h\vec{u}_h, \vec{u}_h)_{0,h} \geq 6\|\vec{u}_h\|_{0,h}^2 > 0$$

if $\vec{u}_h \neq 0 \in \vec{V}_h$. •

5 Discrete Crouzeix-Velte decomposition on a nonequidistant grid in 3D

In this section the well-known difference approximation on a staggered grid will be considered in 3D case, see also [11]. In our case Ω is a rectangular parallelepipedon subdivided by a rectangular grid into $(n-1)(m-1)(l-1)$ cells of volume $h_1h_2h_3$ each, $h_1 := 1/(n-1), h_2 := 1/(m-1), h_3 := 1/(l-1)$. We assume $n, m, l \geq 3$. The cell midpoints are pressure nodes, the pressure vector is denoted by p_h and its components by p_{ijk}, with $i = 1, \dots, n-1$; $j = 1, \dots, m-1$; $k = 1, \dots, l-1$. The faces of the cells contain at their midpoints the velocity nodes: nodes of the u-components of the velocity are on the east-west faces, nodes of the v-components are on the front and back faces and nodes of the w-components are on the north-south faces. The velocity components are denoted by u_{ijk} ($i = 1, \dots, n;\ j = 1, \dots, m-1;\ k = 1, \dots, l-1$), by v_{ijk} ($i = 1, \dots, n-1;\ j = 1, \dots, m;\ k = 1, \dots, l-1$) and by w_{ijk} ($i = 1, \dots, n-1;\ j = 1, \dots, m-1;\ k = 1, \dots, l$). Here the u_{ijk} with $i = 1$ and $i = n$ are the boundary values of u_h; the v_{ijk} with $j = 1$ and $j = m$ are the boundary values of v_h and the w_{ijk} with $k = 1$ and $k = l$ are the boundary values of w_h. The velocity space is $(\mathbb{R}^{nu_h} \times \mathbb{R}^{nv_h} \times \mathbb{R}^{nw_h})$ and will be denoted by $\vec{V}_h$, where $nu_h = n(m-1)(l-1)$, $nv_h = (n-1)m(l-1)$ and $nw_h = (n-1)(m-1)l$. Similarly the pressure space is $\mathbb{R}^{m_h}$ and will be denoted by P_h again, where $m_h = (n-1)(m-1)(l-1)$.

For the approximation of the Stokes problem in 3D we need the discrete divergence operator and the discrete vector Laplace operator. Moreover, we will define also the discrete rotation operator.

The divergence is approximated as follows:

$$(\operatorname{div}_h \vec{u}_h)_{ijk} := \frac{u_{i+1,j,k} - u_{ijk}}{h_1} + \frac{v_{i,j+1,k} - v_{ijk}}{h_2} + \frac{w_{i,j,k+1} - w_{ijk}}{h_3}, \tag{5.1}$$

where

$$\vec{u}_h := (u_h, v_h, w_h)^T;\ \ 1 \leq i \leq n-1,\ \ 1 \leq j \leq m-1,\ \ 1 \leq k \leq l-1.$$

The matrix corresponding to the mapping $-\operatorname{div}_h$ from the velocity space into the pressure space is denoted by $\widetilde{B}_h$ again.

For the approximation of the discrete Laplace operator we continue the grid by lines for u-nodes: $m-1$ lines to north of the cube and $m-1$ lines to south of the cube at a distance $h_3/2$ and $l-1$ lines in front of the cube and behind the cube at a distance $h_2/2$. Similarly we continue the grid by lines for v-nodes north-south and east-west; and for w-nodes front-back and east-west to the cube. Putting zero values into the u-, v- or w-nodes on these lines and using the usual 5-point approximation for the discrete Laplace operator in all inner velocity nodes, we get the following first order approximation:

$$
\begin{aligned}
\Delta_h \vec{u}_h &= (\Delta_h u_h, \Delta_h v_h, \Delta_h w_h)^T, \\
(\Delta_h u_h)_{ijk} &:= \frac{u_{i+1,j,k} - 2u_{ijk} + u_{i-1,j,k}}{h_1^2} + \frac{u_{i,j+1,k} - 2u_{ijk} + u_{i,j-1,k}}{h_2^2} + \\
&+ \frac{u_{i,j,k+1} - 2u_{ijk} + u_{i,j,k-1}}{h_3^2}, \\
& 2 \le i \le n-1, \;\; 1 \le j \le m-1, \;\; 1 \le k \le l-1, \\
(\Delta_h v_h)_{ijk} &:= \frac{v_{i+1,j,k} - 2v_{ijk} + v_{i-1,j,k}}{h_1^2} + \frac{v_{i,j+1,k} - 2v_{ijk} + v_{i,j-1,k}}{h_2^2} + \\
&+ \frac{v_{i,j,k+1} - 2v_{ijk} + v_{i,j,k-1}}{h_3^2}, \\
& 1 \le i \le n-1, \;\; 2 \le j \le m-1, \;\; 1 \le k \le l-1, \\
(\Delta_h w_h)_{ijk} &:= \frac{w_{i+1,j,k} - 2w_{ijk} + w_{i-1,j,k}}{h_1^2} + \frac{w_{i,j+1,k} - 2w_{ijk} + w_{i,j-1,k}}{h_2^2} + \\
&+ \frac{w_{i,j,k+1} - 2w_{ijk} + w_{i,j,k-1}}{h_3^2}, \\
& 1 \le i \le n-1, \;\; 1 \le j \le m-1, \;\; 2 \le k \le l-1.
\end{aligned}
\tag{5.2}
$$

The matrix corresponding to the mapping $-\Delta_h$ from the 3D velocity space into itself is denoted by A_h, as usual. In the case of 3D the discrete rotation operator (rot_h) is a mapping from the velocity space $\vec{V}_h$ into the vector space of the rotation $(\mathbb{R}^{nr})^3$, where $nr = n * m * l$.

$$
(\mathrm{rot}_h\, \vec{u}_h)_{ijk} := \begin{pmatrix} \frac{w_{i,j,k+1} - w_{i,j-1,k+1}}{h_2} - \frac{v_{i,j,k+1} - v_{i,j,k}}{h_3} \\ \frac{u_{i+1,j,k+1} - u_{i+1,j,k}}{h_3} - \frac{w_{i+1,j,k+1} - w_{i,j,k+1}}{h_1} \\ \frac{v_{i+1,j,k} - v_{i,j,k}}{h_1} - \frac{u_{i+1,j,k} - u_{i+1,j-1,k}}{h_2} \end{pmatrix}, \tag{5.3}
$$

where

$$
0 \le i \le n-1, \;\; 1 \le j \le m, \;\; 0 \le k \le l-1.
$$

Once again we use the following notation: $\tilde{C}_h$ for the matrix of the operator rot_h.

5.1 Homogeneous Dirichlet boundary conditions

For pressure vectors p_h, q_h and velocity vectors $\vec{u}_h = (u_h, v_h, w_h)^T$, $\vec{r}_h = (r_h, s_h, t_h)^T$ the following discrete scalar products and the corresponding norms are introduced:

$$(p_h, q_h)_{0,h} := \sum_{i=1}^{n-1}\sum_{j=1}^{m-1}\sum_{k=1}^{l-1} p_{ijk} q_{ijk} h_1 h_2 h_3, \tag{5.4}$$

$$\begin{aligned}(\vec{u}_h, \vec{r}_h)_{0,h} &:= \sum_{i=2}^{n-1}\sum_{j=1}^{m-1}\sum_{k=1}^{l-1} u_{ijk} r_{ijk} h_1 h_2 h_3 + \sum_{i=1}^{n-1}\sum_{j=2}^{m-1}\sum_{k=1}^{l-1} v_{ijk} s_{ijk} h_1 h_2 h_3 + \\ &+ \sum_{i=1}^{n-1}\sum_{j=1}^{m-1}\sum_{k=2}^{l-1} w_{ijk} t_{ijk} h_1 h_2 h_3,\end{aligned} \tag{5.5}$$

$$\|p_h\|_{0,h}^2 := (p_h, p_h)_{0,h}, \quad \|\vec{u}_h\|_{0,h}^2 := (\vec{u}_h, \vec{u}_h)_{0,h}.$$

For the mapping of the operator rot_h: $\vec{u}_h^* = (u_h^*, v_h^*, w_h^*)^T$ and $\vec{r}_h^* = (r_h^*, s_h^*, t_h^*)^T$ we introduce the following scalar product and the corresponding norm:

$$(\vec{u}_h^*, \vec{r}_h^*)_{0,h^*} := \sum_{i=0}^{n-1}\sum_{j=1}^{m}\sum_{k=0}^{l-1} \left(u_{ijk}^* r_{ijk}^* + v_{ijk}^* s_{ijk}^* + w_{ijk}^* t_{ijk}^*\right) h_1 h_2 h_3, \tag{5.6}$$

$$\|\vec{u}_h^*\|_{0,h^*}^2 := (\vec{u}_h^*, \vec{u}_h^*)_{0,h^*}.$$

We assume homogeneous Dirichlet boundary conditions:

$$u_{1,j,k} = u_{n,j,k} = v_{i,1,k} = v_{i,m,k} = w_{i,j,1} = w_{i,j,l} = 0,$$

where $1 \le i \le n-1,\ 1 \le j \le m-1,\ 1 \le k \le l-1$.

Theorem 8

$$(A_h \vec{u}_h, \vec{u}_h)_{0,h} = \|\tilde{B}_h \vec{u}_h\|_{0,h}^2 + \|\tilde{C}_h \vec{u}_h\|_{0,h^*}^2 \tag{5.7}$$

holds for all vectors $\vec{u}_h := (u_h, v_h, w_h)^T$ from the 3D discrete vector space.

Proof. Similar to the two dimensional case we continue the grid functions u_h, v_h and w_h by zero onto the grid of the whole three-dimensional plane and then apply partial summation to $(A_h\vec{u}_h, \vec{u}_h)_{0,h}$ and extend the summation in all expressions to all integer i, j, k. Then we obtain:

$$\begin{aligned}
(A_h\vec{u}_h, \vec{u}_h)_{0,h} &= \sum_{i,j,k} \Big((u_{i+1,j,k} - u_{ijk})^2 \ \frac{h_2 h_3}{h_1} + (u_{i,j+1,k} - u_{ijk})^2 \ \frac{h_1 h_3}{h_2} + \\
&+ \ (v_{i+1,j,k} - v_{ijk})^2 \ \frac{h_2 h_3}{h_1} + (v_{i,j+1,k} - v_{ijk})^2 \ \frac{h_1 h_3}{h_2} + \\
&+ \ (v_{i,j,k+1} - v_{ijk})^2 \ \frac{h_1 h_2}{h_3} + (w_{i+1,j,k} - w_{ijk})^2 \ \frac{h_2 h_3}{h_1} + \\
&+ \ (w_{i,j+1,k} - w_{ijk})^2 \ \frac{h_1 h_3}{h_2} + (w_{i,j,k+1} - w_{ijk})^2 \ \frac{h_1 h_2}{h_3} \Big). \qquad (5.8)
\end{aligned}$$

$\|\tilde{B}_h\vec{u}_h\|^2_{0,h}$ may be written as follows:

$$\begin{aligned}
\|\tilde{B}_h\vec{u}_h\|^2_{0,h} &= \sum_{i,j,k} \Big((u_{i+1,j,k} - u_{ijk})^2 \ \frac{h_2 h_3}{h_1} + \\
&+ \ (v_{i,j+1,k} - v_{ijk})^2 \ \frac{h_1 h_3}{h_2} + (w_{i,j,k+1} - w_{ijk})^2 \ \frac{h_1 h_2}{h_3} + \\
&+ \ 2(u_{i+1,j,k} - u_{ijk})(v_{i,j+1,k} - v_{ijk}) h_3 + \\
&+ \ 2(u_{i+1,j,k} - u_{ijk})(w_{i,j,k+1} - w_{ijk}) h_2 + \\
&+ \ 2(v_{i,j+1,k} - v_{ijk})(w_{i,j,k+1} - w_{ijk}) h_1 \Big). \qquad (5.9)
\end{aligned}$$

$\|\tilde{C}_h\vec{u}_h\|^2_{0,h^*}$ can be written as:

$$\begin{aligned}
\|\tilde{C}_h\vec{u}_h\|^2_{0,h^*} &= \sum_{i,j,k} \Big((w_{i,j,k+1} - w_{i,j-1,k+1})^2 \ \frac{h_1 h_3}{h_2} + (v_{i,j,k+1} - v_{ijk})^2 \ \frac{h_1 h_2}{h_3} - \\
&- \ 2(w_{i,j,k+1} - w_{i,j-1,k+1})(v_{i,j,k+1} - v_{ijk}) h_1 + \\
&+ \ (u_{i+1,j,k+1} - u_{i+1,j,k})^2 \ \frac{h_1 h_2}{h_3} + (w_{i+1,j,k+1} - w_{i,j,k+1})^2 \ \frac{h_2 h_3}{h_1} - \\
&- \ 2(u_{i+1,j,k+1} - u_{i+1,j,k})(w_{i+1,j,k+1} - w_{i,j,k+1}) h_2 + \\
&+ \ (v_{i+1,j,k} - v_{ijk})^2 \ \frac{h_2 h_3}{h_1} + (u_{i+1,j,k} - u_{i+1,j-1,k})^2 \ \frac{h_1 h_3}{h_2} - \\
&- \ 2(v_{i+1,j,k} - v_{ijk})(u_{i+1,j,k} - u_{i+1,j-1,k}) h_3 \Big). \qquad (5.10)
\end{aligned}$$

Performing some index shifts we get the result of Theorem 8. •

5.2 Periodical boundary conditions

Now we consider the staggered grid approximation on a cubic grid. That is, Ω is the unit cube subdivided by a rectangular grid into $(n-1)^3$ cubes of volume h^3 each, $h := 1/(n-1)$. We assume $n \geq 3$.

On the front-back sides and on the north-south sides of the cube we prescribe homogeneous Dirichlet conditions:

$$
\begin{array}{llll}
u_{i,j,0} = u_{i,j,n} = 0 & v_{i,j,0} = v_{i,j,n} = 0 & w_{i,j,1} = w_{i,j,n} = 0 & 1 \leq i, j \leq n-1 \\
u_{i,0,k} = u_{i,n,k} = 0 & v_{i,1,k} = v_{i,n,k} = 0 & w_{i,0,k} = w_{i,n,k} = 0 & 1 \leq i, k \leq n-1
\end{array}
$$

where $u_{i,j,0}, u_{i,j,n}, v_{i,j,0}, v_{i,j,n}$, and $u_{i,0,k}, u_{i,n,k}, w_{i,0,k}, w_{i,n,k}$ are the values on the additional grid lines, as in the previous subsection.

Periodical boundary conditions are assumed on the east-west sides of the unit cube:

$$
\begin{aligned}
u_{1,j,k} &= u_{n-1,j,k}, \quad u_{2,j,k} = u_{n,j,k}, \\
v_{1,j,k} &= v_{n-1,j,k}, \\
w_{1,j,k} &= w_{n-1,j,k},
\end{aligned}
$$

where $1 \leq j, k \leq n-1$.

The approximation of the Laplace operator, the divergence and the rotation are given by (5.2),(5.1) and (5.3) as earlier (now $h_1 = h_2 = h_3 =: h$). The notations A_h, $\tilde{B}_h$ and $\tilde{C}_h$ are the same as earlier, too.

Taking into account the boundary conditions, instead of (5.4),(5.5) and (5.6) we introduce the following scalar products and norms:

$$(p_h, q_h)_{0,h} := \sum_{i=1}^{n-2} \sum_{j,k=1}^{n-1} p_{ijk} q_{ijk} h^3, \tag{5.11}$$

$$\begin{aligned}(\vec{u}_h, \vec{r}_h)_{0,h} &:= \sum_{i=2}^{n-1} \sum_{j=1}^{n-1} \sum_{k=1}^{n-1} u_{ijk} r_{ijk} h^3 + \sum_{i=1}^{n-2} \sum_{j=2}^{n-1} \sum_{k=1}^{n-1} v_{ijk} s_{ijk} h^3 + \\ &+ \sum_{i=1}^{n-2} \sum_{j=1}^{n-1} \sum_{k=2}^{n-1} w_{ijk} t_{ijk} h^3,\end{aligned} \tag{5.12}$$

$$\begin{aligned}(\vec{u}_h^*, \vec{r}_h^*)_{0,h^*} &:= \sum_{i=1}^{n-2} \sum_{j=1}^{n} \sum_{k=0}^{n-1} u^*_{ijk} r^*_{ijk} h^3 + \sum_{i=0}^{n-3} \sum_{j=1}^{n-1} \sum_{k=0}^{n-1} v^*_{ijk} s^*_{ijk} h^3 + \\ &+ \sum_{i=0}^{n-3} \sum_{j=1}^{n} \sum_{k=1}^{n-1} w^*_{ijk} t^*_{ijk} h^3\end{aligned} \tag{5.13}$$

$$\|p_h\|^2_{0,h} := (p_h, p_h)_{0,h}, \quad \|\vec{u}_h\|^2_{0,h} := (\vec{u}_h, \vec{u}_h)_{0,h}, \quad \|\vec{u_h^*}\|^2_{0,h^*} := (\vec{u}_h^*, \vec{u}_h^*)_{0,h^*}.$$

Using these scalar products and norms we obtain:

Theorem 9

$$(A_h \vec{u}_h, \vec{u}_h)_{0,h} = \|\tilde{B}_h \vec{u}_h\|^2_{0,h} + \|\tilde{C}_h \vec{u}_h\|^2_{0,h^*} \tag{5.14}$$

holds for all vectors $\vec{u}_h := (u_h, v_h, w_h)^T$ from the 3D discrete vector space.

Proof.
Using partial summation to $(A_h \vec{u}_h, \vec{u}_h)_{0,h}$ we obtain:

$$
\begin{aligned}
(A_h\vec{u}_h,\vec{u}_h)_{0,h} &= \sum_{i=1}^{n-2}\sum_{j=1}^{n-1}\sum_{k=1}^{n-1} h(u_{i+1,j,k}-u_{ijk})^2 + \sum_{i=2}^{n-1}\sum_{j=1}^{n-2}\sum_{k=1}^{n-1} h(u_{i,j+1,k}-u_{ijk})^2 + \\
&+ \sum_{i=2}^{n-1}\sum_{k=1}^{n-1} h(u_{i,n-1,k}^2+u_{i,1,k}^2) + \sum_{i=2}^{n-1}\sum_{j=1}^{n-1}\sum_{k=1}^{n-2} h(u_{i,j,k+1}-u_{ijk})^2 + \\
&+ \sum_{i=2}^{n-1}\sum_{j=1}^{n-1} h(u_{i,j,n-1}^2+u_{i,j,1}^2) + \sum_{i=0}^{n-3}\sum_{j=2}^{n-1}\sum_{k=1}^{n-1} h(v_{i+1,j,k}-v_{ijk})^2 + \\
&+ \sum_{i=1}^{n-2}\sum_{j=2}^{n-2}\sum_{k=1}^{n-1} h(v_{i,j+1,k}-v_{ijk})^2 + \sum_{i=1}^{n-2}\sum_{k=1}^{n-1} h(v_{i,n-1,k}^2+v_{i,2,k}^2) + \\
&+ \sum_{i=1}^{n-2}\sum_{j=2}^{n-1}\sum_{k=1}^{n-2} h(v_{i,j,k+1}-v_{ijk})^2 + \sum_{i=1}^{n-2}\sum_{j=2}^{n-1} h(v_{i,j,n-1}^2+v_{i,j,1}^2) + \\
&+ \sum_{i=0}^{n-3}\sum_{j=1}^{n-1}\sum_{k=2}^{n-1} h(w_{i+1,j,k}-w_{ijk})^2 + \sum_{i=1}^{n-2}\sum_{j=1}^{n-2}\sum_{k=2}^{n-1} h(w_{i,j+1,k}-w_{ijk})^2 + \\
&+ \sum_{i=1}^{n-2}\sum_{k=2}^{n-1} h(w_{i,n-1,k}^2+w_{i,1,k}^2) + \sum_{i=1}^{n-2}\sum_{j=1}^{n-1}\sum_{k=2}^{n-2} h(w_{i,j,k+1}-w_{ijk})^2 + \\
&+ \sum_{i=1}^{n-2}\sum_{j=1}^{n-1} h(w_{i,j,n-1}^2+w_{i,j,2}^2). \qquad (5.15)
\end{aligned}
$$

$\|\tilde{B}_h\vec{u}_h\|_{0,h}^2$ may be written as:

$$
\begin{aligned}
\|\tilde{B}_h\vec{u}_h\|_{0,h}^2 &= \sum_{i=1}^{n-2}\sum_{j=1}^{n-1}\sum_{k=1}^{n-1} h(u_{i+1,j,k}-u_{ijk})^2 + \sum_{i=1}^{n-2}\sum_{j=1}^{n-1}\sum_{k=1}^{n-1} h(v_{i,j+1,k}-v_{ijk})^2 + \\
&+ \sum_{i=1}^{n-2}\sum_{j=1}^{n-1}\sum_{k=1}^{n-1} h(w_{i,j,k+1}-w_{ijk})^2 + \qquad (5.16) \\
&+ 2\sum_{i=1}^{n-2}\sum_{j=1}^{n-1}\sum_{k=1}^{n-1} h(u_{i+1,j,k}-u_{ijk})(v_{i,j+1,k}-v_{ijk}) + \\
&+ 2\sum_{i=1}^{n-2}\sum_{j=1}^{n-1}\sum_{k=1}^{n-1} h(u_{i+1,j,k}-u_{ijk})(w_{i,j,k+1}-w_{ijk}) + \\
&+ 2\sum_{i=1}^{n-2}\sum_{j=1}^{n-1}\sum_{k=1}^{n-1} h(v_{i,j+1,k}-v_{ijk})(w_{i,j,k+1}-w_{ijk}).
\end{aligned}
$$

For $\|\tilde{C}_h\vec{u}_h\|^2_{0,h^*}$ we get:

$$\begin{aligned}
\|\tilde{C}_h\vec{u}_h\|^2_{0,h^*} \;=\;& \sum_{i=1}^{n-2}\sum_{j=1}^{n}\sum_{k=0}^{n-1} h\Big((w_{i,j,k+1}-w_{i,j-1,k+1})^2+(v_{i,j,k+1}-v_{ijk})^2\Big) - \\
-\;& 2\sum_{i=1}^{n-2}\sum_{j=1}^{n}\sum_{k=0}^{n-1} h(w_{i,j,k+1}-w_{i,j-1,k+1})(v_{i,j,k+1}-v_{ijk}) + \\
+\;& \sum_{i=0}^{n-3}\sum_{j=1}^{n-1}\sum_{k=0}^{n-1} h\Big((u_{i+1,j,k+1}-u_{i+1,j,k})^2+(w_{i+1,j,k+1}-w_{i,j,k+1})^2\Big) - \\
-\;& 2\sum_{i=0}^{n-3}\sum_{j=1}^{n-1}\sum_{k=0}^{n-1} h(u_{i+1,j,k+1}-u_{i+1,j,k})(w_{i+1,j,k+1}-w_{i,j,k+1}) + \\
+\;& \sum_{i=0}^{n-3}\sum_{j=1}^{n}\sum_{k=1}^{n-1} h\Big((v_{i+1,j,k}-v_{i,j,k})^2+(u_{i+1,j,k}-u_{i+1,j-1,k})^2\Big) - \\
-\;& 2\sum_{i=0}^{n-3}\sum_{j=1}^{n}\sum_{k=1}^{n-1} h(v_{i+1,j,k}-v_{i,j,k})(u_{i+1,j,k}-u_{i+1,j-1,k}). \qquad (5.17)
\end{aligned}$$

Performing some index shifts and taking into account the Dirichlet and periodical boundary conditions we obtain the result of Theorem 9. •

Remark For the dimension of $\ker \operatorname{div}_h$ and $\ker \operatorname{rot}_h$, see [11]. The result of Theorem 3. can be also generalized to 3D. •

6 The Crouzeix-Velte decomposition and the Stokes problem in polar coordinates for the disk domain

Let Ω be the unit disk

$$\Omega = \{(r,\varphi)|0 \le r < 1, 0 \le \varphi < 2\pi\},$$

and consider the following Stokes problem:

$$\Delta_{r\varphi} u - \frac{u}{r^2} - \frac{2}{r^2}\frac{\partial v}{\partial \varphi} - \frac{\partial p}{\partial r} \quad = \quad f_1, \tag{6.1}$$

$$\Delta_{r\varphi} v - \frac{v}{r^2} + \frac{2}{r^2}\frac{\partial u}{\partial \varphi} - \frac{1}{r}\frac{\partial p}{\partial \varphi} \quad = \quad f_2, \tag{6.2}$$

$$\operatorname{div}\vec{u} = \frac{1}{r}\left(\frac{\partial}{\partial r}(ru) + \frac{\partial v}{\partial \varphi}\right) \quad = \quad 0, \tag{6.3}$$

where $(u,v) = \vec{u}$ and $(f_1, f_2) = \vec{f}$ and

$$\Delta_{r\varphi} = \frac{1}{r}\frac{\partial}{\partial r}\left(r\frac{\partial}{\partial r}\right) + \frac{1}{r^2}\frac{\partial^2}{\partial \varphi^2}.$$

On the boundary, homogeneous Dirichlet boundary conditions are imposed:

$$\vec{u} = 0, \text{ on } \partial\Omega. \tag{6.4}$$

The problem consists in finding a vector-function $\vec{u}(x)$ and a scalar function $p(x)$ that satisfy the system of partial differential equations above. In (6.1)-(6.2), the differential operator acting on, $\vec{u}$ is nothing else than the Laplace-operator in polar coordinates, see (6.12) below. We mention that the appearance of v in the equation (6.1) and the appearance of u in the equation (6.2) cause difficulties during the numerical solution of (6.1)-(6.4).

If $-\operatorname{div}\vec{u} = g$ in (6.3) and the boundary conditions are inhomogeneous, than the solvability condition of (6.1)-(6.3):

$$\int_\Omega g dx = -\int_\Omega \operatorname{div}\vec{u} dx = -\int_\Gamma \vec{u}\vec{n} ds. \tag{6.5}$$

has to be also satisfied.

For existence and uniqueness of the classical solution see [18].

The analytical case of the Crouzeix-Velte decomposition for two-dimensional domains was investigated, and for the circle domain, the spectrum of the Schur complement was proved to be $0, 1/2, 1$, where $1/2$ and 1 have infinite multiplicity, in [7], [13] and [8].

The results of the spectrum for tube domains are contained in [12]. A three-dimensional ball is considered in [31].

6.1 The staggered grid approximation on a unit disk

The difference approximation on a staggered grid will be considered here: Ω is the unit disk subdivided by an equidistant grid according to r and φ into n*m cells. The cell midpoints are pressure nodes, the pressure vector is denoted by p_h and its components by p_{ij}, with $i = 1, \ldots, n; j = 1, \ldots, m$. The sides of the cells contain as their midpoints the velocity nodes: nodes of the u-components of the velocity are on the sides according to r, nodes of the v-components are on the sides according to φ. The velocity vector is $\vec{u}_h$, its components are denoted by u_h and v_h and theirs components by u_{ij} and $v_{ij},\ i = 1, \ldots, n,\ \ j = 1, \ldots, m$. The boundary values are $u_{n,j} := 0$ where $j = 1, \ldots, m$, further u_h and v_h are periodical with respect to φ, that is

$$u_{i,0} = u_{i,m}, \ \ v_{i,0} = v_{i,m}, \ \ i = 1, \ldots, n, \tag{6.6}$$

see Figure 2.

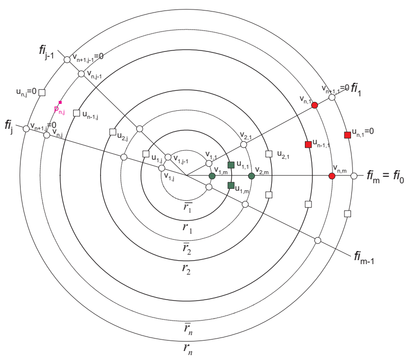

Figure 2: Staggered grid approximation on a unit disk

For the approximation of the Stokes problem we need the discrete gradient, the discrete divergence operator and the vector Laplace operator. Moreover, we will also define the discrete rotation and curl operators. For the gradient:

$$(\operatorname{grad} p) = \begin{pmatrix} \frac{\partial p}{\partial r} \\ \frac{1}{r}\frac{\partial p}{\partial \varphi} \end{pmatrix} \tag{6.7}$$

we shall use the approximation:

$$(\mathrm{grad}_h\, p_h)_{ij} := \begin{pmatrix} (p_{i+1,j} - p_{i,j})/h_r \\ \frac{1}{\overline{r}_i}(p_{i,j+1} - p_{i,j})/h_\varphi \end{pmatrix} \tag{6.8}$$

where $h_r := 1/n$, $h_\varphi := 1/m$ and $\overline{r}_i := (i{-}1/2)h_r$, $i = 1, \ldots, n$, $j = 1, \ldots, m$. For the approximation of the divergence operator, we shall use:

$$(\mathrm{div}_h\, \vec{u}_h)_{ij} := \frac{r_i u_{i,j} - r_{i-1}u_{i-1,j}}{\overline{r}_i h_r} + \frac{v_{i,j} - v_{i,j-1}}{\overline{r}_i h_\varphi}, \tag{6.9}$$

where $r_i := ih_r$, $i = 1, \ldots, n$, $j = 1, \ldots, m$ and $r_0 u_{0,j} = 0$. (To approximate the divergence we used the grid points marked with red colour on Figure 2.)

For the rotation:

$$(\mathrm{rot}\, \vec{u}) = \frac{1}{r}\left(\frac{\partial}{\partial r}(rv) - \frac{\partial u}{\partial \varphi}\right) \tag{6.10}$$

we shall use the approximation:

$$(\mathrm{rot}_h\, \vec{u}_h)_{ij} := \frac{\overline{r}_{i+1}v_{i+1,j} - \overline{r}_i v_{i,j}}{r_i h_r} - \frac{u_{i,j+1} - u_{i,j}}{r_i h_\varphi}, \tag{6.11}$$

where $i = 1, \ldots, n-1$, $j = 1, \ldots, m$, and

$$(\mathrm{rot}_h\, \vec{u}_h)_{nj} := \frac{\overline{r}_n v_{n,j}}{r_n h_r/2}$$

where $j = 1, \ldots, m$. (See grid points marked with green on Figure 2.)

For scalar functions, we define the operator curl as follows:

$$(\mathrm{curl}\, \psi) := \begin{pmatrix} \frac{1}{r}\frac{\partial \psi}{\partial \varphi} \\ -\frac{\partial \psi}{\partial r}, \end{pmatrix}$$

and we shall approximate this operator in the following way:

$$(\mathrm{curl}_h\, \psi)_{ij} := \begin{pmatrix} \frac{1}{r_i}\frac{\psi_{ij} - \psi_{i,j-1}}{h_\varphi} \\ -\frac{\psi_{ij} - \psi_{i-1,j}}{h_r}, \end{pmatrix}$$

Since

$$(\mathrm{grad}\,\mathrm{div}\,\vec{u} - \mathrm{curl}\,\mathrm{rot}\,\vec{u}) = \begin{pmatrix} \frac{\partial}{\partial r}\left(\frac{1}{r}\frac{\partial}{\partial r}(ru) + \frac{1}{r}\frac{\partial v}{\partial \varphi}\right) - \frac{1}{r}\frac{\partial}{\partial \varphi}\left(\frac{1}{r}\frac{\partial}{\partial r}(rv) - \frac{1}{r}\frac{\partial u}{\partial \varphi}\right) \\ \frac{1}{r}\frac{\partial}{\partial \varphi}\left(\frac{1}{r}\frac{\partial}{\partial r}(ru) + \frac{1}{r}\frac{\partial v}{\partial \varphi}\right) + \frac{\partial}{\partial r}\left(\frac{1}{r}\frac{\partial}{\partial r}(rv) - \frac{1}{r}\frac{\partial u}{\partial \varphi}\right) \end{pmatrix},$$

that is

$$(\operatorname{grad}\operatorname{div}\vec{u} - \operatorname{curl}\operatorname{rot}\vec{u}) = \left(\begin{array}{c} \frac{1}{r}\frac{\partial}{\partial r}\left(r\frac{\partial u}{\partial r}\right) - \frac{u}{r^2} - \frac{2}{r^2}\frac{\partial v}{\partial \varphi} + \frac{1}{r^2}\frac{\partial^2 u}{\partial \varphi^2} \\ \frac{1}{r}\frac{\partial}{\partial r}\left(r\frac{\partial v}{\partial r}\right) - \frac{v}{r^2} + \frac{2}{r^2}\frac{\partial u}{\partial \varphi} + \frac{1}{r^2}\frac{\partial^2 v}{\partial \varphi^2} \end{array} \right),$$

the identity (2.24) holds in polar coordinate system in the following form:

$$\left(\begin{array}{c} \Delta_{r\varphi} u - \frac{u}{r^2} - \frac{2}{r^2}\frac{\partial v}{\partial \varphi} \\ \Delta_{r\varphi} v - \frac{v}{r^2} + \frac{2}{r^2}\frac{\partial u}{\partial \varphi} \end{array} \right) = (\operatorname{grad}\operatorname{div}\vec{u} - \operatorname{curl}\operatorname{rot}\vec{u}) = \Delta\vec{u}. \tag{6.12}$$

Using the identity (6.12) and the approximation of the divergence (6.9), rotation (6.11) and curl (6.12), we can approximate the Stokes problem (6.1) - (6.4) as follows:

$$\left(\begin{array}{cc} \tilde{A}_h & \tilde{B}_h^T \\ \tilde{B}_h & 0 \end{array} \right) \left(\begin{array}{c} \vec{u} \\ p \end{array} \right) = \left(\begin{array}{c} \vec{f} \\ 0 \end{array} \right), \tag{6.13}$$

where $\tilde{B}_h$ corresponds to the negative divergence operator and $\tilde{A}_h$ corresponds to the negative Laplace operator, i.e. the left side of the identity (6.12) and is the following:

$$\begin{aligned} -(\tilde{A}_h \vec{u}_h)_{ij} &:= \frac{1}{h_r}\Big(\frac{1}{\overline{r}_{i+1}}((ru)_r)_{i+1,j} - \frac{1}{\overline{r}_i}((ru)_r)_{i,j}\Big) + \\ &+ \frac{1}{h_r}\Big(\frac{1}{\overline{r}_{i+1}}(v_\varphi)_{i+1,j} - \frac{1}{\overline{r}_i}(v_\varphi)_{i,j}\Big) + \\ &+ \frac{1}{h_\varphi r_i^2}\left((u_\varphi)_{i,j+1} - (u_\varphi)_{i,j}\right) - \\ &- \frac{1}{h_\varphi r_i^2}\left(((\overline{r}v)_{\overline{r}})_{i+1,j} - ((\overline{r}v)_{\overline{r}})_{i+1,j-1}\right) \end{aligned} \tag{6.14}$$

$$\begin{aligned} -(\tilde{A}_h \vec{v}_h)_{ij} &:= \frac{1}{h_r}\Big(\frac{1}{r_i}((\overline{r}v)_{\overline{r}})_{i+1,j} - \frac{1}{r_{i-1}}((\overline{r}v)_{\overline{r}})_{i,j}\Big) + \\ &+ \frac{1}{h_r}\Big(\frac{1}{r_{i-1}}(u_\varphi)_{i-1,j+1} - \frac{1}{r_i}(u_\varphi)_{i,j+1}\Big) + \\ &+ \frac{1}{h_\varphi \overline{r}_i^2}\left((v_\varphi)_{i,j+1} - (v_\varphi)_{i,j}\right) - \\ &- \frac{1}{h_\varphi \overline{r}_i^2}\left(((ru)_r)_{i,j+1} - ((ru)_r)_{i,j}\right), \end{aligned} \tag{6.15}$$

where $i = 1, \ldots, n,\ \ j = 1, \ldots, m$ and taking into account (6.6), and we used the following notations:

$$
\begin{aligned}
(u_\varphi)_{i,j} &:= \frac{u_{i,j} - u_{i,j-1}}{h_\varphi}, \\
(v_\varphi)_{i,j} &:= \frac{v_{i,j} - v_{i,j-1}}{h_\varphi}, \\
((ru)_r)_{i,j} &:= \frac{r_i u_{i,j} - r_{i-1} u_{i-1,j}}{h_r}, \\
((\overline{r}v)_{\overline{r}})_{i,j} &:= \frac{\overline{r}_i v_{i,j} - \overline{r}_{i-1} v_{i-1,j}}{h_r}.
\end{aligned}
\tag{6.16}
$$

We also introduce the following notation: $\tilde{C}_h$ for the matrix of the operator rot_h.

For pressure vectors p_h, q_h and velocity vectors $\vec{u}_h = (u_h, v_h)^T$, $\vec{w}_h = (t_h, s_h)^T$ the following discrete scalar products and the corresponding norms are introduced:

$$
\begin{aligned}
(p_h, q_h)_{0,\overline{r},h} &:= \sum_{i=1}^{n} \sum_{j=1}^{m} p_{ij} q_{ij} \overline{r}_i h_r h_\varphi, \qquad (6.17) \\
\|p_h\|^2_{0,\overline{r},h} &:= (p_h, p_h)_{0,\overline{r},h},
\end{aligned}
$$

and

$$
\begin{aligned}
(p_h, q_h)_{0,r,h} &:= \sum_{i=1}^{n} \sum_{j=1}^{m} p_{ij} q_{ij} r_i h_r h_\varphi, \qquad (6.18) \\
\|p_h\|^2_{0,r,h} &:= (p_h, p_h)_{0,r,h},
\end{aligned}
$$

and

$$
\begin{aligned}
(\vec{u}_h, \vec{w}_h)_{0,h} &:= \sum_{i=1}^{n} \sum_{j=1}^{m} (u_{ij} t_{ij} r_i + v_{ij} s_{ij} \overline{r}_i) h_r h_\varphi \qquad (6.19) \\
\|\vec{u}_h\|^2_{0,h} &:= (\vec{u}_h, \vec{u}_h)_{0,h}.
\end{aligned}
$$

Theorem 10

$$
(\tilde{A}_h \vec{u}_h, \vec{u}_h)_{0,h} = \|\tilde{B}_h \vec{u}_h\|^2_{0,\overline{r},h} + \|\tilde{C}_h \vec{u}_h\|^2_{0,r,h} \tag{6.20}
$$

holds for all vectors $\vec{u}_h := (u_h, v_h)^T \in \vec{V}_h$

Proof.

We apply partial summation to $(\tilde{A}_h\vec{u}_h, \vec{u}_h)_{0,h}$:

$$
\begin{aligned}
(\tilde{A}_h\vec{u}_h, \vec{u}_h)_{0,h} = & \sum_{i=1}^{n-1}\sum_{j=1}^{m} \frac{h_\varphi}{\overline{r}_{i+1}h_r}(r_{i+1}u_{i+1,j} - r_i u_{i,j})^2 + \\
+ & \sum_{j=1}^{m} \frac{h_\varphi}{\overline{r}_1 h_r}(r_1 u_{1,j})^2 + \sum_{i=1}^{n}\sum_{j=1}^{m} \frac{h_r}{r_i h_\varphi}(u_{i,j+1} - u_{i,j})^2 - \\
- & \sum_{i=1}^{n}\sum_{j=1}^{m} \Big(\frac{r_i}{\overline{r}_{i+1}}(v_{i+1,j}u_{i,j} - v_{i+1,j-1}u_{i,j}) - \frac{r_i}{\overline{r}_i}(v_{i,j}u_{i,j} - v_{i,j-1}u_{i,j}) \Big) - \\
- & \sum_{i=1}^{n}\sum_{j=1}^{m} \Big(\frac{\overline{r}_{i+1}}{r_i}(v_{i+1,j-1}u_{i,j} - v_{i+1,j}u_{i,j}) - \frac{\overline{r}_i}{r_i}(v_{i,j-1}u_{i,j} - v_{i,j}u_{i,j}) \Big) + \\
+ & \sum_{i=1}^{n-1}\sum_{j=1}^{m} \frac{h_\varphi}{r_i h_r}(\overline{r}_{i+1}v_{i+1,j} - \overline{r}_i v_{i,j})^2 + \qquad (6.21) \\
+ & \sum_{j=1}^{m} \frac{h_\varphi}{r_n h_r}(\overline{r}_n v_{n,j})^2 + \sum_{i=1}^{n}\sum_{j=1}^{m} \frac{h_r}{\overline{r}_i h_\varphi}(v_{i,j+1} - v_{i,j})^2 - \\
- & \sum_{i=1}^{n}\sum_{j=1}^{m} \Big(\frac{\overline{r}_i}{r_{i-1}}(u_{i-1,j+1}v_{i,j} - u_{i-1,j}v_{i,j}) - \frac{\overline{r}_i}{r_i}(u_{i,j+1}v_{i,j} - u_{i,j}v_{i,j}) \Big) - \\
- & \sum_{i=1}^{n}\sum_{j=1}^{m} \Big(\frac{r_{i-1}}{\overline{r}_i}(u_{i-1,j}v_{i,j} - u_{i-1,j+1}v_{i,j}) - \frac{r_i}{\overline{r}_i}(u_{i,j}v_{i,j} - u_{i,j+1}v_{i,j}) \Big).
\end{aligned}
$$

$\|\tilde{B}_h\vec{u}_h\|^2_{0,\overline{r},h}$ may be written in the following form:

$$
\begin{aligned}
\|\tilde{B}_h\vec{u}_h\|^2_{0,\overline{r},h} = & \sum_{i=1}^{n}\sum_{j=1}^{m} \Big(\frac{h_\varphi}{\overline{r}_i h_r}(r_i u_{i,j} - r_{i-1}u_{i-1,j})^2 + \qquad (6.22) \\
+ & \frac{h_r}{\overline{r}_i h_\varphi}(v_{i,j} - v_{i,j-1})^2 + \frac{2}{\overline{r}_i}(r_i u_{i,j} - r_{i-1}u_{i-1,j})(v_{i,j} - v_{i,j-1}) \Big).
\end{aligned}
$$

$\|\tilde{C}_h\vec{u}_h\|^2_{0,r,h}$ can be written as follows:

$$
\begin{aligned}
\|\tilde{C}_h\vec{u}_h\|^2_{0,r,h} = & \sum_{i=1}^{n}\sum_{j=1}^{m} \Big(\frac{h_r}{r_i h_\varphi}(u_{i,j+1} - u_{i,j})^2 + \frac{h_\varphi}{r_i h_r}(\overline{r}_{i+1}v_{i+1,j} - \overline{r}_i v_{i,j})^2 - \\
- & \frac{2}{r_i}(u_{i,j+1} - u_{i,j})(\overline{r}_{i+1}v_{i+1,j} - \overline{r}_i v_{i,j}) \Big). \qquad (6.23)
\end{aligned}
$$

Performing some index shifts and taking into account the periodicity in the direction φ and the homogeneous boundary conditions we get:

$$(\tilde{A}_h\vec{u}_h, \vec{u}_h)_{0,h} - \|\tilde{B}_h\vec{u}_h\|^2_{0,\overline{r},h} - \|\tilde{C}_h\vec{u}_h\|^2_{0,r,h} = 0. \quad \bullet$$

Remark $\tilde{A}_h$ is a symmetric matrix in the sense of the scalar product (6.19). This means that (6.20) can be described in matrix terms as follows:

$$\begin{aligned}(D_{\tilde{A}}\tilde{A}_h\vec{u}_h,\vec{u}_h) &= (D_{\tilde{B}}\tilde{B}_h\vec{u}_h,\tilde{B}_h\vec{u}_h)+(D_{\tilde{C}}\tilde{C}_h\vec{u}_h,\tilde{C}_h\vec{u}_h)= \\ &= (\tilde{B}_h^T D_{\tilde{B}}\tilde{B}_h\vec{u}_h,\vec{u}_h)+(\tilde{C}_h^T D_{\tilde{C}}\tilde{C}_h\vec{u}_h,\vec{u}_h),\end{aligned} \tag{6.24}$$

where (.,.) is the Euclidean scalar product and $D_{\tilde{A}}, D_{\tilde{B}}, D_{\tilde{A}}$ are diagonal matrices corresponding to (6.19), (6.17) and (6.18):

$$\begin{aligned}D_{\tilde{A}} &= diag\,(r_1 I_{m\times m},...,r_{n-1}I_{m\times m},\overline{r}_1 I_{m\times m},...,\overline{r}_n I_{m\times m})\,h_r h_\varphi, \\ D_{\tilde{B}} &= diag\,(\overline{r}_1 I_{m\times m},...,\overline{r}_n I_{m\times m},)\,h_r h_\varphi, \\ D_{\tilde{C}} &= diag\,(r_1 I_{m\times m},...,r_n I_{m\times m},)\,h_r h_\varphi.\end{aligned} \tag{6.25}$$

From (6.24) we obtain:

$$D_{\tilde{A}}\tilde{A}_h = \tilde{B}_h^T D_{\tilde{B}}\tilde{B}_h + \tilde{C}_h^T D_{\tilde{C}}\tilde{C}_h. \tag{6.26}$$

That is $D_{\tilde{A}}\tilde{A}_h$ is a symmetric matrix and can be written in the following form:

$$D_{\tilde{A}}\tilde{A}_h =: A_h = B_h + C_h, \tag{6.27}$$

where $B_h = \hat{B}_h^T\hat{B}_h$ and $C_h = \hat{C}_h^T\hat{C}_h$ with the notation $\hat{B}_h = D_{\tilde{B}}^{1/2}\tilde{B}_h, \hat{C}_h = D_{\tilde{C}}^{1/2}\tilde{C}_h$.
•

6.2 Numerical results

Using the notations (6.27) our problem consists in finding the solution of the following algebraic system:

$$A_h\vec{u}_h + \hat{B}_h^T p_h = \vec{f}_h, \tag{6.28}$$
$$\hat{B}_h\vec{u}_h = g_h. \tag{6.29}$$

We use the Uzawa-algorithm ([2]) to solve (6.28), (6.29):

$$\begin{aligned} p_h^{(0)} &:= 0, \\ p_h^{(i+1)} &:= p_h^{(i)} + \omega(\hat{B}_h\vec{u}_h^{(i)} - g_h) \\ \vec{u}_h^{(i)} &:= A_h^{-1}(\vec{f}_h - \hat{B}_h^T p_h^{(i)}) \\ i = 0, 1, 2, \ldots . & \end{aligned} \tag{6.30}$$

(6.30) can be written in the following form:

$$\begin{aligned} p_h^{(0)} &= 0, \\ p_h^{(i+1)} &= p_h^{(i)} + \omega(\psi_h - S_h p_h^{(i)}) \\ i = 0, 1, 2, \ldots . & \end{aligned} \tag{6.31}$$

where $\psi_h = \hat{B}_h A_h^{-1}\vec{f}_h - g_h$ and S_h is the discrete Schur complement operator, that is $S_h = \hat{B}_h A_h^{-1}\hat{B}_h^T$. Since the discrete Crouzeix-Velte decomposition exists, using the Uzawa-algorithm we can reach the third Crouzeix-Velte subspace after 1 step, if $p_0 = 0$ ([23]). In this subspace the spectrum of the Schur complement is closer, and the algorithm shows effective convergence. We introduce the following notations: the optimal iteration parameter is $\omega_{opt}^h := 2/(\underline{\lambda}_h + \bar{\lambda}_h)$, where $\underline{\lambda}_h$ and $\overline{\lambda}_h$ are the smallest and the largest of the eigenvalues different from 0 and 1 of the discrete Schur complement; and $\omega = 2$ is the optimal iteration parameter for the undiscretized Uzawa-algorithm, see ([23]). Table 1 shows the values of the optimal iteration parameter (ω_{opt}^h) and the smallest and largest eigenvalues ($\underline{\lambda}_h, \overline{\lambda}_h$).

Table 1

$n = m$	5	10	20	40	60
$\underline{\lambda}_h$	0.5133234	0.5036472	0.5009311	0.5002340	0.5001041
$\overline{\lambda}_h$	0.5248821	0.5188427	0.5154488	0.5138629	0.5133509
ω_{opt}^h	1.926401	1.95601	1.967768	1.972198	1.973447

In a first numerical experiment in (6.28), (6.29) we took random values for the exact solution p_h which was projected to the orthogonal complement of the kernel of $\hat{B}_h^T$. Here ψ_h was calculated as $\psi_h := S_h p_h$. After $i = 1, 2$ initial steps with $\omega = 1$, the optimal parameters have been taken. In Table 2 $\langle i; \omega_{opt}^h \rangle$ means the number of iterations (including the initial steps using $\omega = 1$ iteration parameter) in the case of i initial steps and after that iterations with ω_{opt}^h. $\langle i; \omega = 2\rangle$ means the number of iterations in the case of i initial steps followed by iterations with $\omega = 2$. For comparison we show the number of iterations in the case of $\omega = 1$ iteration parameter in all steps - which is in widespread use - denoted by $\langle 1; \omega = 1 \rangle$. The numerical convergence rate $q := (\|e^{(it)}\| / \|e^{(0)}\|)^{1/it}$ is also shown, where $e^{(0)}$ is the initial pressure error and $e^{(it)}$ is the final error after it iterations. The stopping criterion is that the initial pressure error in the Euclidean norm has been reduced by a factor of 10^{-5}. The numerical experiments showed that in the inner iteration (in the conjugate gradient method, for details see below) it is necessary to use a stronger stopping criterion: that the initial error in the Euclidean norm has been decreased at least by a factor of 10^{-6}. (If in the outer iteration the initial pressure error is reduced by a factor of 10^{-10} than in the inner iteration it is necessary to decrease the initial error at least by a factor of 10^{-11}.)

Table 2

$n = m$	5	10	20	40	60
$\langle 1; \omega = 1 \rangle$	14	15	16	17	17
q	0.4179	0.4172	0.4131	0.4166	0.4129
$\langle 1; \omega_{opt}^h \rangle$	4	4	4	4	4
q	0.0056	0.0057	0.0046	0.0041	0.0041
$\langle 1; \omega = 2 \rangle$	5	4	4	4	4
q	0.0291	0.0138	0.0105	0.0090	0.0083
$\langle 2; \omega_{opt}^h \rangle$	4	5	5	5	5
q	0.0029	0.0044	0.0041	0.0034	0.0032
$\langle 2; \omega = 2 \rangle$	5	5	5	5	5
q	0.0144	0.0106	0.0090	0.0074	0.0067

In the second numerical experiment, an algebraic Stokes problem with known solution has been generated. (The exact solution is: $u_{exact} = r \cos \varphi + 2r \sin \varphi + 3$, $v_{exact} = 4r \cos \varphi - r \sin \varphi + 2$ and $p_{exact} = 2r \cos \varphi$. In this case $\operatorname{div}(u, v) = 0$ and the solvability condition of (6.28), (6.29) - the discrete equivalent of (6.5) - is satisfied.) The number of outer iterations and the numerical convergence rate are shown in Table 3 depending on the iteration parameter. Here, iteration was stopped if the initial pressure error had been reduced by a factor of 10^{-6}. In the inner iteration the initial error in the Euclidean norm has been decreased by a factor of 10^{-7}.

Table 3

$n = m$	5	10	20	40	60	80
$\langle 1; \omega = 1 \rangle$	21	22	23	24	25	25
q	0.4693	0.5022	0.5606	0.5784	0.6354	0.6143
$\langle 1; \omega^h_{opt} \rangle$	5	5	5	5	5	-
q	0.0341	0.0690	0.0742	0.0932	0.0110	-
$\langle 1; \omega = 2 \rangle$	5	4	4	4	3	3
q	0.0342	0.0283	0.0312	0.0422	0.0043	0.00731
$\langle 2; \omega^h_{opt} \rangle$	5	6	6	6	6	-
q	0.0112	0.0690	0.0742	0.0932	0.0092	-
$\langle 2; \omega = 2 \rangle$	6	5	5	4	4	4
q	0.0341	0.0283	0.0312	0.0087	0.0043	0.0073

Because of the large amount of memory needed, ω^h_{opt} was not calculated in the case of $n = m = 80$. Let us point out that, the speed of convergence is growing together with the refinement of the grid - except when $\omega = 1$ in all steps.

Instead of the calculation of A_h^{-1} in (6.30) we investigated two solutions. In the first case we used the fast Fourier transformation in combination with the preconditioned conjugate gradient method and in the second case we used the multigrid method.

6.2.1 Fourier transformation and conjugate gradient method

For calculation of A_h^{-1} with Fourier transformation and the conjugate gradient method, let us introduce the following notations:

$$\begin{aligned} \vec{u}_{h,F} &:= Q^*_{2n-1}\vec{u}_h, & p_{h,F} &:= Q^*_n p_h, \\ A_{h,F} &:= Q^*_{2n-1} A_h Q_{2n-1}, & \hat{B}_{h,F} &:= Q^*_n \hat{B}_h Q_{2n-1}, \end{aligned} \tag{6.32}$$

where Q_k, the matrix of the Fourier transformation, is a block-diagonal matrix with k blocks $Q = (q_{j,l})^m_{j,l=1}$ and $q_{j,l} = \sqrt{1/m}\; e^{ih_\varphi lj}$. Now, instead of (6.30), the following iteration for the transformed variables can be used:

$$\vec{f}_{h,F} := Q^*_{2n-1}\vec{f}_h, \qquad g_{h,F} := Q^*_n g_h, \qquad \text{(FFT)} \tag{6.33}$$

$$p^{(0)}_{h,F} := 0,$$

$$\Big[p^{(i+1)}_{h,F} := p^{(i)}_{h,F} + \omega(\hat{B}_{h,F}\vec{u}^{(i)}_{h,F} - g_{h,F}) \tag{6.34}$$

$$A_{h,F}\; \vec{u}^{(i)}_{h,F} := \vec{f}_{h,F} - \hat{B}^*_{h,F} p^{(i)}_{h,F} \Big] \tag{6.35}$$

$$i = 0, 1, 2, \ldots .$$

$$\vec{u}_h := Q_{2n-1}\vec{u}_{h,F}, \qquad p_h := Q_n p_{h,F}, \qquad \text{(IFFT)}. \tag{6.36}$$

Observe that in a cartesian coordinate system, $A_{h,F}$ would be block-diagonal with tridiagonal blocks. In our case of polar coordinates, however, $A_{h,F}$ has 7 nonzero diagonals, the main diagonal, the $\pm m$-th, the $\pm(m-1)*n$-th and the $\pm(m-1)*n+m$-th diagonal (using the Matlab notation). To solve (6.35) approximately in an inner iteration, the preconditioned conjugate gradient method was used combined with incomplete Gauss-elimination. (Additional diagonals were not used in the incomplete Gauss-elimination. This version is sometimes called ILU(0).) In the numerical experiments several ILU(0)-type preconditioning matrices fitting to the structure of $A_{h,F}$ were investigated and T_{opt} was found to be the optimal preconditioner from the 5 preconditioners considered, resulting in the fastest convergence with few number of iterations.

T_{opt} is a tridiagonal matrix consisting of the main diagonal and the m-th and $-m$-th diagonal of $A_{h,F}$. In the previous numerical experiments, this preconditioning matrix was used.

Table 4 displays the number of inner iterations needed to reach the stopping criterion of the conjugate gradient method, in that the initial error in the Euclidean norm has been decreased by a factor of 10^{-4}. In the table T_{opt} shows that the matrix T_{opt} was used as the preconditioning matrix.

The unpreconditioned conjugate gradient method is denoted by $T = I$.

For comparison we show the number of iterations with three further preconditioning matrices:
T_D contains only the main diagonal of $A_{h,F}$,
T_* is a tridiagonal matrix consisting of the main diagonal and the $(m-1)*n+m$-th and $-((m-1)*n+m)$-th diagonal of $A_{h,F}$ and
T_{**} is a pentadiagonal matrix with the main diagonal and the $\pm m$-th and $\pm(m-1)*n+m$-th diagonal of $A_{h,F}$.

Table 4

$n=m$	5	10	20	50	100	200	500	640
T_{opt}	9	12	12	12	8	5	5	4
$T=I$	25	59	76	197	362	-	-	-
T_D	19	39	72	106	125	-	-	-
T_*	19	39	72	107	125	-	-	-
T_{**}	7	8	8	8	5	3	2	2

Because of the large amount of computational time needed, the preconditioning matrices: $T = I$, T_D and T_* were not used in the case of $n = m \geq 200$.

In Table 5 we show the computational time of the conjugate gradient method (inner iteration) to reach our stopping criterion 10^{-4}, and the necessary additional memory for the incomplete Gauss-elimination using the different preconditioning matrices and $n = m = 50$.

Table 5

$n = m = 50$	computational time (s)	additional memory needed (byte)
T_{opt}	32.3	2400
$T = I$	202.7	-
T_D	163.9	800
T_*	326.5	2400
T_{**}	63.9	4000

The full computational time of the second numerical experiment in the case of $\langle 1; \omega = 2\rangle$ and $n = m = 50$ is the following: the time of the FFT and IFFT and the calculation of ψ_h are altogether $25,2\ s$ and the full time of the outer iteration (see (6.34), $max_{it} = 3$) is $121.1\ s$. Here the stopping criterion of the inner iteration is 10^{-4} and the stopping criterion of the outer iteration is 10^{-3} and we used T_{opt} as the preconditioning matrix.

6.2.2 Multigrid method

Instead of the use of fast Fourier transformation in combination with the preconditioned conjugate gradient method , we can apply the multigrid method for solving

$$\begin{aligned} A_h \vec{u}_h^{(i)} &= (\vec{f}_h - \hat{B}_h^T p_h^{(i)}) := \vec{b}_h \\ i = 0, 1, 2, \ldots . \end{aligned} \tag{6.37}$$

in the Uzawa algorithm (6.30), where $\vec{b}_h = (b_h^{(u)}, b_h^{(v)})$.

We define a coarse and a fine grid on the Ω domain (ω_H and ω_h) and we approximate $\vec{u}_h^{(i)}$ on the fine grid. The well-known algorithm of the two-grid method is the following (see [16], [27]):

$\vec{y}_h^{(0)}$	given initial iterate of $\vec{u}_h^{(i)}$,
$\vec{y}_h^{(j)} := S_h^{\nu_1}(A_h, \vec{b}_h)\vec{y}_h^{(j)}$	application of ν_1 pre-smoothing iterations to $\vec{y}^{(j)}$
$\vec{r}_h^{(j)} := \vec{b}_h - A_h \vec{y}_h^{(j)}$	calculation of the defect
$\vec{r}_H^{(j)} := R_h^H \vec{r}_h^{(j)}$	restriction of the defect, R_h^H is the restriction operator
$\vec{w}_H^{(j)} := A_H^{-1} \vec{r}_H^{(j)}$	solution of the coarse-grid equation
$\vec{w}_h^{(j)} := P_H^h \vec{w}_H^{(j)}$	interpolation of $\vec{w}_H^{(j)}$, P_H^h is the prolongation operator
$\vec{y}_h^{(j+1)} := \vec{y}_h^{(j)} + \vec{w}_h^{(j)}$	correction of $\vec{y}_h$
$\vec{y}_h^{(j+1)} := S_h^{\nu_2}(A_h, \vec{b}_h)\vec{y}_h^{(j+1)}$	application of ν_2 post-smoothing iterations to $\vec{y}^{(j+1)}$
$j = 0, 1, 2, \ldots .$	

In our case for the coarse grid the unit circle is subdivided by an equidistant r, φ-grid into n*m cells. For the fine grid, the unit circle is subdivided into 2n*2m cells. This grid is also equidistant and every second grid lines fit to the grid lines of the coarse grid. To use the two-grid and later the multigrid method we need to define the restriction from the fine to the coarse grid and the method of prolongation that prescribes the interpolation from the coarse to the fine grid. We remark that in the case of staggered grid approximation the u and v-values on the coarse grid do not fit to the fine grid.

We used the following weighted restriction: let $u^H_{i,j}$ denote a value of the u velocity component on the coarse grid. To calculate u^H_{ij} we use 6 u-values on the fine grid. 2 u-values are on the same radius r_i where u^H_{ij} is, adjacent to u^H_{ij}. The weights of these u-values are $\frac{1}{4}$. Moreover 4 u-values are on the radii $\overline{r}_i$ and $\overline{r}_{i+1}]$ of the coarse grid, their weights are $\frac{1}{8}$. That is

$$\begin{aligned} u^H_{i,j} &= \frac{1}{4}(u_{2i,2j} + u_{2i,2j-1}) + \\ &+ \frac{1}{8}(u_{2i-1,2j} + u_{2i-1,2j-1} + u_{2i+1,2j} + u_{2i+1,2j-1}). \end{aligned} \tag{6.38}$$

where $u_{i,j}$ is a value of the u velocity component on the fine grid, see the blue points in Figure 3, where the bold lines denote the grid lines of the coarse grid.

Similarly, for calculation of v^H_{ij} on the coarse grid we also take into account 6 v-values on the fine grid. 2 v-values are on the same grid line according to φ where v^H_{ij} is, adjacent to v^H_{ij}. Their weights are $\frac{1}{4}$. And 4 v-values are on the next grid lines according to φ of the fine grid (these grid lines do not appear as a line of the coarse grid). Their weights are $\frac{1}{8}$. That is

$$\begin{aligned} v^H_{i,j} &= \frac{1}{4}(v_{2i,2j} + v_{2i-1,2j}) + \\ &+ \frac{1}{8}(v_{2i,2j-1} + v_{2i-1,2j-1} + v_{2i,2j+1} + v_{2i-1,2j+1}). \end{aligned} \tag{6.39}$$

where $v_{i,j}$ denotes a value of the v velocity component on the fine grid, see also the red points in Figure 3, where we used the notation i', j' instead of i and j.

Let R^H_h be the matrix of the restriction operator. It is a rectangular $N_H \times N_h$ matrix, where $N_H = (n-1) * m + n * m$ and $N_h = (2n-1) * 2m + 2n * 2m$. E.g. if $n = m = 2$ then R^H_h will be the following:

$$R^H_h = \frac{1}{8} \begin{pmatrix} 1&1&&&2&2&&&1&1&&&&&&&&&&&&&&&&&& \\ &&1&1&&&2&2&&&1&1&&&&&&&&&&&&&&&& \\ &&&&&&&&&&&&2&1&&1&2&1&&1&&&&&&&& \\ &&&&&&&&&&&&&1&2&1&&1&2&1&&&&&&&& \\ &&&&&&&&&&&&&&&&&&&&2&1&&1&2&1&&1 \\ &&&&&&&&&&&&&&&&&&&&&1&2&1&&1&2&1 \end{pmatrix}$$

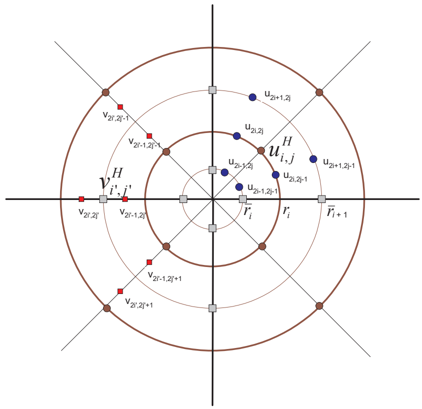

Figure 3: Restriction on the unit disk

The most difficult task was to find a good interpolation for the two-grid (or multigrid) method. The reason of the difficulties is the singularity in the centre of the disk which causes big oscillations of the defect on the innermost circles, see Figure 4 and Figure 5 (here the number of grid lines on the fine grid are $2n = 2m = 32$).

For finite different-based multigrid, a general formula for interpolation is the following [stoyan, personal communication]:

$$P_H^h = (D_{\tilde{A}}^H \ R_h^H \ (D_{\tilde{A}}^h)^{-1})^T$$

where $D_{\tilde{A}}^H$ is the diagonal matrix (6.24) corresponding to the scalar product (6.19) on the coarse grid and $D_{\tilde{A}}^h$ is the same diagonal matrix on the fine grid, R_h^H is the matrix of the restriction operator. The numerical experiments showed that the multigrid method is non convergent using this interpolation if the refinement of the grid is large ($n = m \geq 64$). We found that the multigrid method is convergent with the interpolation:

$$P_H^h = c \ (D_{\tilde{A}}^H \ R_h^H \ (D_{\tilde{A}}^h)^{-1})^T, \tag{6.40}$$

where $0 < c < 1$ constant. Choosing appropriate values of c, we have minimized the norm of the final error after 30 full iteration steps of the multigrid method. We used the Matlab fmins function for the minimization. The result of the minimization see later, in Table 6.

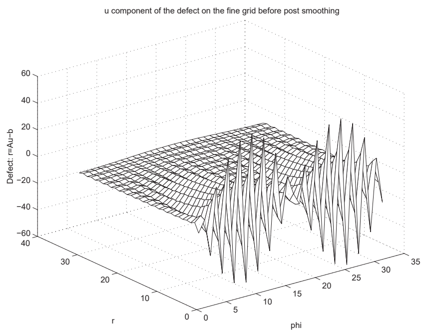

Figure 4: Oscillation of the defect related to the u velocity component

Moreover, for the two-grid (or multigrid) method we will also need a smoothing iteration. For the often used damped Jacobi iteration we can estimate the optimal smoothing iteration parameter:

Theorem 11 The optimal iteration parameter of damped Jacobi iteration is approximately

$$\omega \approx \frac{12h_r^2 h_\varphi^2}{30h_\varphi^2 + 54h_r + 35h_r h_\varphi} \tag{6.41}$$

where $h_r := 1/n$ and $h_\varphi := 1/m$.

Proof. We choose the ω iteration parameter from the following requirement:

$$1 > 1 - \omega\lambda_{N_1} = -(1 - \omega\lambda_{N_h}) > -1 \tag{6.42}$$

where λ_{N_1} is the $N_H + 1 =: N_1$th eigenvalue and $\lambda_{N_h} := \lambda_{max}$ is the N_hth eigenvalue of A_h. Here N_H is the number of points of the coarse ω_H grid and N_h is the number of points of the fine grid ω_h.

From (6.42) we get:

$$\omega = \frac{2}{\lambda_{N_1} + \lambda_{N_h}}. \tag{6.43}$$

The λ_{N_1} and λ_{N_h} eigenvalues can be estimated by the maximum norm:

$$\lambda_{N_h} \approx \|A_h\|_{C(\omega_h)},$$
$$\lambda_{N_1} \approx \lambda_{N_H} \approx \|A_H\|_{C(\omega_H)},$$

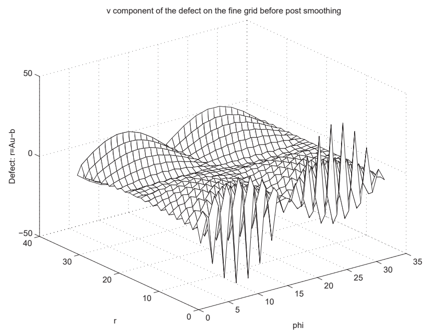

Figure 5: Oscillation of the defect related to the v velocity component

where λ_{N_H} is the largest of the eigenvalues of A_H.

From (6.14), (6.15) and (6.25), (6.27) we get:

$$\begin{aligned}
(A_h\vec{u}_h)_{ij} := & \left(\frac{r_i^2}{h_r^2\overline{r}_{i+1}} + \frac{r_i^2}{h_r^2\overline{r}_i} + \frac{2}{h_\varphi^2 r_i}\right) u_{ij} - \frac{r_i r_{i+1}}{h_r^2\overline{r}_{i+1}} u_{i+1,j} - \\
- & \frac{r_i r_{i-1}}{h_r^2\overline{r}_i} u_{i-1,j} - \frac{1}{h_\varphi^2 r_i}(u_{i,j+1} + u_{i,j-1}) + \\
+ & \left(\frac{r_i}{h_r h_\varphi \overline{r}_i} - \frac{\overline{r}_i}{h_r h_\varphi r_i}\right)(v_{ij} - v_{i,j-1}) + \\
+ & \left(-\frac{r_i}{h_r h_\varphi \overline{r}_{i+1}} + \frac{\overline{r}_{i+1}}{h_r h_\varphi r_i}\right)(v_{i+1,j} - v_{i+1,j-1}), \qquad (6.44)
\end{aligned}$$

$$\begin{aligned}
(A_h\vec{v}_h)_{ij} := & \left(\frac{\overline{r}_i^2}{h_r^2 r_{i-1}} + \frac{\overline{r}_i^2}{h_r^2 r_i} + \frac{2}{h_\varphi^2 \overline{r}_i}\right) v_{ij} - \frac{\overline{r}_i \overline{r}_{i+1}}{h_r^2 r_i} v_{i+1,j} - \\
- & \frac{\overline{r}_i \overline{r}_{i-1}}{h_r^2 r_{i-1}} v_{i-1,j} - \frac{1}{h_\varphi^2 \overline{r}_i}(v_{i,j+1} + v_{i,j-1}) + \\
+ & \left(\frac{r_i}{h_r h_\varphi \overline{r}_i} - \frac{\overline{r}_i}{h_r h_\varphi r_i}\right)(u_{ij} - u_{i,j+1}) + \\
+ & \left(-\frac{\overline{r}_i}{h_r h_\varphi r_{i-1}} + \frac{r_{i-1}}{h_r h_\varphi \overline{r}_i}\right)(u_{i-1,j+1} - u_{i-1,j}), \qquad (6.45)
\end{aligned}$$

where $i = 1, \ldots, 2n, \;\; j = 1, \ldots, 2m.$

From (6.44) and (6.45) the maximum norm of A_h can be estimated in the following form:

$$\begin{aligned}\|A_h\|_{C(\omega_h)} \ \ &\leq max\Big[\tfrac{1}{h_r^2}\left(\tfrac{r_i^2}{\overline{r}_{i+1}}+\tfrac{r_i^2}{\overline{r}_i}+\tfrac{r_ir_{i+1}}{\overline{r}_{i+1}}+\tfrac{r_{i-1}r_i}{\overline{r}_i}\right)+\\ &\qquad +\tfrac{4}{h_\varphi^2 r_i}+\tfrac{2}{h_rh_\varphi}\left(\tfrac{r_i^2-\overline{r}_i^2}{r_i\overline{r}_i}+\tfrac{\overline{r}_{i+1}^2-r_i^2}{r_i\overline{r}_{i+1}}\right);\\ &\qquad \tfrac{1}{h_r^2}\left(\tfrac{\overline{r}_i^2}{r_i}+\tfrac{\overline{r}_i^2}{r_{i-1}}+\tfrac{\overline{r}_i\overline{r}_{i+1}}{r_i}+\tfrac{\overline{r}_{i-1}\overline{r}_i}{r_{i-1}}\right)+\\ &\qquad +\tfrac{4}{h_\varphi^2\overline{r}_i}+\tfrac{2}{h_rh_\varphi}\left(\tfrac{r_i^2-\overline{r}_i^2}{r_i\overline{r}_i}+\tfrac{\overline{r}_i^2-r_{i-1}^2}{r_{i-1}\overline{r}_i}\right)\Big].\end{aligned} \tag{6.46}$$

Since $r_i = ih_r$ and $\overline{r}_i = (i-\frac{1}{2})h_r$, the following estimations can be proved:

$$\begin{aligned}\frac{r_i^2-\overline{r}_i^2}{r_i\overline{r}_i}+\frac{\overline{r}_{i+1}^2-r_i^2}{r_i\overline{r}_{i+1}} \ &= \ \frac{i^2-(i-\frac{1}{2})^2}{i(i-\frac{1}{2})}+\frac{(i+\frac{1}{2})^2-i^2}{(i+\frac{1}{2})i}\leq\\ &\leq \ \frac{(i-\frac{1}{4})}{(i-\frac{1}{2})}+\frac{(i+\frac{1}{4})}{(i+\frac{1}{2})}\leq\frac{7}{3}\end{aligned} \tag{6.47}$$

and

$$\begin{aligned}&\tfrac{r_i^2}{\overline{r}_{i+1}}+\tfrac{r_i^2}{\overline{r}_i}+\tfrac{r_ir_{i+1}}{\overline{r}_{i+1}}+\tfrac{r_{i-1}r_i}{\overline{r}_i}=\\ ih_r&\left(\tfrac{i(i-\frac{1}{2})+i(i+\frac{1}{2})+(i+1)(i-\frac{1}{2})+(i-1)(i+\frac{1}{2})}{(i+\frac{1}{2})(i-\frac{1}{2})}\right)\leq 4,\end{aligned} \tag{6.48}$$

using that $ih_r \leq 1$ and

$$\frac{(i+\frac{1}{2})(2i-1)+(i-\frac{1}{2})(2i+1)}{(i+\frac{1}{2})(i-\frac{1}{2})}=4.$$

Moreover

$$\frac{r_i^2-\overline{r}_i^2}{r_i\overline{r}_i}+\frac{\overline{r}_i^2-r_{i-1}^2}{r_{i-1}\overline{r}_i} \ = \ \frac{(i-\frac{1}{4})}{i(i-\frac{1}{2})}+\frac{(i-\frac{3}{4})}{i^2-\frac{3}{2}i+\frac{1}{2}}\leq\frac{3}{2} \tag{6.49}$$

and

$$\frac{\overline{r}_i^2}{r_i}+\frac{\overline{r}_i^2}{r_{i-1}}+\frac{\overline{r}_i\overline{r}_{i+1}}{r_i}+\frac{\overline{r}_{i-1}\overline{r}_i}{r_{i-1}}=ih_r\left(\frac{4i^2-6i+2}{i(i-1)}\right)\leq 4. \tag{6.50}$$

From (6.47) - (6.50) we obtain:

$$\|A_h\|_{C(\omega_h)} \quad \leq \tfrac{4}{h_r^2} + \tfrac{4}{h_\varphi^2 \overline{r}_i} + \tfrac{14}{3h_r h_\varphi} \leq \tfrac{12h_\varphi^2+24h_r+14h_r h_\varphi}{3h_r^2 h_\varphi^2}. \tag{6.51}$$

Since on the coarse grid the grid spacings are: $H_r := 2h_r$ and $H_\varphi := 2h_\varphi$, from (6.51) we can estimate the maximum norm of A_H in the following way:

$$\|A_H\|_{C(\omega_H)} \quad \leq \tfrac{12H_\varphi^2+24H_r+14H_r H_\varphi}{3H_r^2 H_\varphi^2} = \tfrac{6h_\varphi^2+6h_r+7h_r h_\varphi}{6h_r^2 h_\varphi^2}. \tag{6.52}$$

From (6.43),(6.51) and (6.52) we can calculate the optimal iteration parameter, ω.

•

Remark The convergence rate (q) of the smoothing Jacobi iteration with the optimal ω parameter is estimated as follows:

$$\frac{3}{5} \leq q = \frac{\lambda_{N_h} - \lambda_{N_H}}{\lambda_{N_h} + \lambda_{N_H}} = \frac{1 - \frac{\lambda_{N_H}}{\lambda_{N_h}}}{1 + \frac{\lambda_{N_H}}{\lambda_{N_h}}} \leq \frac{7}{9},$$

since

$$\frac{1}{8} \leq \frac{\lambda_{N_H}}{\lambda_{N_h}} = \frac{6h_\varphi^2 + 6h_r + 7h_r h_\varphi}{24h_\varphi^2 + 48h_r + 28h_r h_\varphi} \leq \frac{1}{4}. \quad \bullet$$

Figure 6 shows the norm of the defect, $\|r_h\|_{C(\omega_h)} := \|b_h - A_h y_h\|_{C(\omega_h)}$, on the fine grid after one full step of the two-grid method. Here and in the following numerical experiments $\vec{b}_h = (\vec{f}_h - \hat{B}_h^T p_{exact})$, where $p_{exact} = 2r\cos\varphi$, $\vec{f}_h = 0$, as it was described in the second numerical experiment related to the Uzawa-algorithm. The pre- and post smoothing iteration is damped Jacobi iteration with variable iteration parameter ω. The number of Jacobi iterations is 20, that is $\nu_1 = \nu_2 = 20$, for the fine grid the domain is subdivided into 128*128 cells. The optimal iteration parameter calculated by (6.41) is $3.477 * 10^{-6}$. The figure displays that the norm of the defect is really almost the smallest using the calculated optimal iteration parameter. It is displayed also that the two-grid method is not convergent in this case if the iteration parameter is greater than $4.5 * 10^{-6}$.

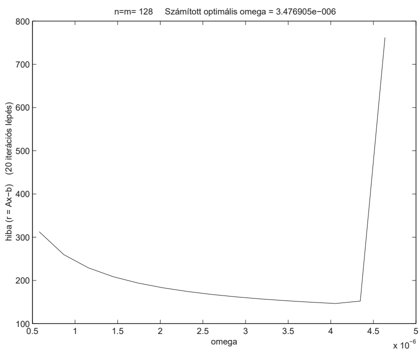

Figure 6: Investigation of the optimal iteration parameter of the damped Jacobi iteration

In the numerical experiments the damped Jacobi iteration with the optimal parameter ω and the Gauss-Seidel iteration were investigated and compared as smoothing iteration and Gauss-Seidel iteration was found to be the better one, resulting into faster convergence and smoothing with the same number of iterations. To smooth faster the oscillations in the centre of the disk we combined the Gauss-Seidel iteration with a block-Gauss-Seidel step: we calculated the velocity values on the innermost circle exactly using the already calculated (approximate) values on the neighbouring circle for it. If we calculate the values exactly on the innermost circle, using (6.44) and (6.45) we have to solve the following equation system:

$$
\begin{aligned}
(\breve{A}_h u_h)_j &:= \left(\frac{r_1^2}{h_r^2\overline{r}_2} + \frac{r_1^2}{h_r^2\overline{r}_1} + \frac{2}{h_\varphi^2 r_1}\right) u_{1,j} - \frac{1}{h_\varphi^2 r_1}(u_{1,j+1} + u_{1,j-1}) + \\
&+ \left(\frac{r_1}{h_r h_\varphi \overline{r}_1} - \frac{\overline{r}_1}{h_r h_\varphi r_1}\right)(v_{1,j} - v_{1,j-1}) = \\
&= b_h(1,j)^{(u)} + \frac{r_1 r_2}{h_r^2 \overline{r}_2} u_{2,j} - \left(-\frac{r_1}{h_r h_\varphi \overline{r}_2} + \frac{\overline{r}_2}{h_r h_\varphi r_1}\right)(v_{2,j} - v_{2,j-1}) := f_{h,j}^{(u)}
\end{aligned}
$$

$$(\breve{A}_h v_h)_j := \left(\frac{\overline{r}_1^2}{h_r^2 r_1} + \frac{2}{h_\varphi^2 \overline{r}_1}\right) v_{1,j} - \frac{1}{h_\varphi^2 \overline{r}_1}(v_{1,j+1} + v_{1,j-1}) +$$
$$+ \left(\frac{r_1}{h_r h_\varphi \overline{r}_1} - \frac{\overline{r}_1}{h_r h_\varphi r_1}\right)(u_{1,j} - u_{1,j+1}) =$$
$$= b_h(1,j)^{(v)} + \frac{\overline{r}_1 \overline{r}_2}{h_r^2 r_1} v_{2,j} := f_{h,j}^{(v)}$$

Here $\breve{A}_h$ is a matrix of dimension $4m$ on the fine grid ($2m$ on the coarse grid) in contrast to the dimension of A_h, which is $N_h = (2n-1)*2m+2n*2m$ on the fine grid ($N_H = (n-1)*m + n*m$ on the coarse grid).

On Figure 7 we compared the decrease of the defect during the post-smoothing, using different type of iterations. Here we applied not the two-grid, but the multi-grid method (see: [27], [16]), with three levels and the defect was investigated on the highest level, after one full step of the multi-grid method. On the figure the dotted line signs the norm of the defect using the Jacobi-iteration with optimal parameter ω, the solid line shows the Gauss-Seidel iteration and the dashdot shows one step with Gauss-Seidel and one block-Gauss-Seidel step on the innermost circle, in turns. The figure displays that the Gauss-Seidel iteration resulted faster convergence (together with smoothing) as the Jacobi iteration, moreover the Gauss-Seidel iteration is faster when combined with block-Gauss-Seidel steps. The numerical experiments showed that it is enough to have only one block-Gauss-Seidel step after the first Gauss-Seidel iteration step for the faster convergence.

Table 6 displays the number of full iteration steps of the multigrid method (the number of μ) needed to reach the stopping criterion, that the initial error of the solution of (6.37) in the Euclidean norm be decreased by a factor of 10^{-4}, where the initial error is $e^{(0)} := \vec{y}^{(0)} - A_h^{-1}\vec{b}_h$. (*nc* means that the iteration is not convergent).

In the table *it.type* $= J$ shows that the smoothing iteration was the damped Jacobi-iteration with the calculated optimal iteration parameter ω; if *it.type* $= GS$ than the Gauss-Seidel iteration was used as smoothing iteration and finally *it.type* $= GS + BGS$ means that the Gauss-Seidel iteration was combined with a block-Gauss-Seidel step.

Minimizing the final error, $e^{(\mu)} = e^{(30)}$ after $\mu = 30$ full iteration steps, we calculated the optimal constant c in (6.40). Table 6 displays the value of the optimal c depending on the refinement of the grid, if the method is the two-grid method and the smoothing iteration is the Gauss-Seidel iteration combined with a block-Gauss-Seidel step denoted by c_{opt}^{GS}. We calculated

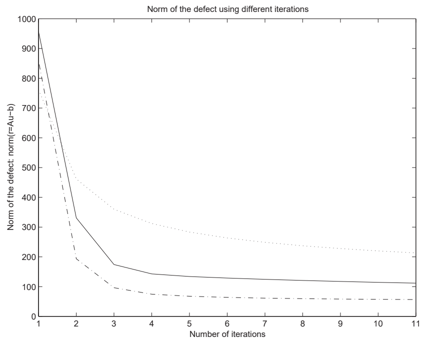

Figure 7: Comparison of the post-smoothing iterations

the optimal constant c in the case, if the method is the two-grid method and the smoothing iteration is the Jacobi iteration as well, this constant is denoted by c^J_{opt}. (The optimal constant was not calculated with the other smoothing iterations and other number of the levels of the multigrid method. Some numerical experiments showed that it does not cause relevant difference in the number of iteration steps needed to reach the stopping criterion.) For comparison in the last two rows of the table we display the number of iterations needed in the cases of $c = 0.5$ and $c = 1$. Moreover l_{max} shows the number of the levels of the multigrid method and $\nu_1 = \nu_2 = 5$ is the number of the pre- and post-smoothing iterations. We used the W-cycle multigrid iteration - which proved to be faster -, but for comparison, in the last column of the table the results calculated by V-cycle iteration are shown, in the case of $n = m = 128$.

The results show that the Gauss-Seidel iteration combined with block Gauss-Seidel iteration - as smoothing iteration - is the most effective: the multigrid method using this iteration is on average 5-8 times faster than using the Gauss-Seidel iteration and this advantage is growing with the refinement of the grid. The less effective smoothing iteration is the Jacobi iteration, it results on average three times slower convergence than the Gauss-Seidel iteration.

Table 6

$n=m$		8	16	32	64	128	128
c_{opt}^{GS}		0.9900	0.9400	0.7844	0.6879	0.6225	
l_{max}	*it.type*						
2	GS	10	14	27	82	300	300
2	GS+BGS	5	7	9	11	24	24
3	GS	-	14	37	105	382	nc
3	GS+BGS	-	7	10	14	25	27
4	GS	-	-	45	123	426	nc
4	GS+BGS	-	-	10	15	26	44
c_{opt}^{J}		0.6800	0.5779	0.6450	0.6531	-	
l_{max}	*it.type*						
2	J	25	32	76	234	-	
$c=0.5$							
2	J	30	34	85	238	-	
2	GS+BGS	8	13	15	16	25	
$c=1$							
2	J	nc	nc	nc	nc	nc	
2	GS+BGS	5	7	12	nc	nc	

In Table 7 we show the number of iterations and the computational time of the multigrid method to reach our stopping criterion 10^{-4} using different smoothing iterations with their optimal constant c_{opt} and different levels of the multigrid method, $n=m=48$.

Table 7

$n=m=48$			
l_{max}	*it.type*	number of it.	comp. time (s)
2	GS	64	385.6
2	GS+BGS	11	59.2
2	J	148	1423.6
3	GS	64	570.4
3	GS+BGS	14	99.6
3	J	170	2668.4
4	GS	76	767.1
4	GS+BGS	15	117.9
4	J	203	3101.1

The computational time of the multigrid method with Gauss-Seidel iteration combined with a block Gauss-Seidel step in the case of $n=m=50, \nu_1=\nu_2=3$ is $65.3s$. Comparing it with the conjugate gradient method, it seems that the multigrid method is a bit slower than the conjugate gradient method with the optimal preconditioning matrix, T_{opt} ($57.4s$ together with FFT and IFFT), but it is faster than the conjugate gradient method with the second best preconditioning matrix, T_{**} ($89.1s$), and substantially faster than the conjugate gradient method with other preconditioning matrices.

7 Summary

In our dissertation we dealt with the numerical solution of the Stokes problem. First we described the Stokes problem in a cartesian coordinate system and introduced the analytical, the algebraic and the discrete Crouzeix-Velte decompositions.

After that the first order staggered grid approximation was investigated in 2D case, on a non-equidistant rectangular grid, with homogeneous Dirichlet boundary conditions, using finite difference- and finite volume methods. In these cases we gave the conditions of the existence of the discrete Crouzeix-Velte decomposition. These results are for domains composed of rectangles. We showed with numerical experiments - using the approximation based on the finite volume method - that both the Uzawa-type and the conjugate gradient-type methods are faster on such grids which are condensing in the center and coarser near the boundary of the domain.

Afterwards we considered the second order staggered grid approximation on an equdistant grid in the unit square using finite difference method, where the boundary conditions were homogeneous Dirichlet boundary conditions. We proved that in this case the Crouzeix-Velte decomposition exists not for the matrix of the negative Laplace operator but for an analogous matrix, which hence can be advantageous as a preconditional matrix.

Then we proved the existence of the Crouzeix-Velte decomposition in the case of special non-standard and periodical boundary conditions: in the first case the Crouzeix-Velte decomposition exists using both first and second order staggered grid approximations, in the second case this decomposition exists using only first order approximation. We generalized our results to the 3D case as well.

Finally we described the Stokes problem in a polar coordinate system and the existence of the discrete Crouzeix-Velte decomposition for the unit disk was proved in the case of second order staggered grid approximation.

The numerical experiments proved that the approximation giving rise to a discrete Crouzeix–Velte decomposition leads to effectively solvable systems of algebraic equations using the Uzawa algorithm. To solve the discrete Poisson equations on the unit disk, the conjugate gradient method and the multigrid method was applied and in the first case the most effective preconditioning matrix, in the second case the most efficient smoothing iteration was also described.

8 Összefoglalás

Disszertációnkban a Stokes feladat numerikus megoldásával foglalkoztunk. Bevezetésként bemutattuk a Stokes feladatot Descartes-féle koordináta rendszerben és definiáltuk az analitikus-, az algebrai- és a diszkrét Crouzeix-Velte -féle felbontás fogalmát.

Elsőként elsőrendű approximációkat vizsgáltunk két dimenziós esetben az eltolt rácsrendszeren, nemekvidisztans rácsot figyelembe véve, homogén Dirichlet peremfeltételek mellett. Használtunk véges differencia- és véges térfogat approximációkat is. A vizsgált esetekben megadtuk a diszkrét Crouzeix-Velte -féle felbontás létezésének feltételeit. Ezek az eredmények kiterjeszthetők téglalapokból összeállított tartományok esetére is. Numerikus kísérletekkel igazoltuk - véges térfogat módszert használva-, hogy mind az Uzawa-típusú, mind a konjugált gradiens típusú módszerek gyorsabbak az olyan nemekvidisztans rácsokon, melyek sűrűbbek a tartomány belseje felé haladva és ritkábbak a perem közelében.

Ezután másodrendű approximációt vizsgáltunk ekvidisztans rácson, egységnégyzet tartományban, véges differencia módszert alkalmazva, homogén Dirichlet peremfeltétel mellett. Bizonyítottuk, hogy ebben az esetben a Crouzeix-Velte -féle felbontás nem a negatív Laplace-operátorra vonatkozóan létezik, hanem egy hozzá hasonló (tőle csak a perempontokban eltérő) mátrixra vonatkozóan, amely mátrix ilyen módon előnyös szerepet játszhat, mint prekondicionáló mátrix.

A továbbiakban speciális nemstandard valamint periodikus peremfeltételeket vizsgáltunk és bizonyítottuk ezek esetén a diszkrét Crouzeix-Velte -féle felbontás létezését: a nemstandard peremfeltételek esetén a Crouzeix-Velte -féle felbontás mind első-, mind másodrendű approximáció esetén létezik, míg periodikus peremfeltételeket figyelembe véve a felbontás létezése csak elsőrendű approximáció esetén bizonyítható.

Eredményeinket általánosítottuk három dimenziós tartomány esetére is.

Végül definiáltuk a Stokes feladatot polárkoordináta rendszerben és bizonyítottuk a diszkrét Crouzeix-Velte -féle felbontás létezését egységkör tartományon, az eltolt rácsrendszerre illeszkedő másodrendű véges differencia approximáció esetén.

Számos numerikus kísérletet végeztünk, amelyek igazolták, hogy a diszkrét Crouzeix-Velte -féle felbontást eredményező approximáció Uzawa – algoritmussal hatékonyan megoldható egyenletrendszerhez vezet. A diszkrét Poisson egyenlet megoldására az egységkörön két módszert is alkalmaztunk: egyrészt a konjugált gradiens módszert, melynek esetén meghatároztuk a leghatékonyabban működő prekondicionáló mátrixot; másrészt a többrácsos módszert, melynek esetén különböző simító iterációkat hasonlítottunk össze és mutattuk be a leghatékonyabbat.

References

[1] ADAMS R.A.: *Sobolev Spaces*. Academic Press, New York, (1975).

[2] ARROW K., HURWICZ L., UZAWA H.: *Studies in Linear and Nonlinear Programming*. Stanford University Press, Stanford, (1958).

[3] AGMON, S., DOUGLIS, A., NIRENBERG, L.: *Estimates near the boundary for solutions of elliptic partial differential equations satisfying general boundary conditions* II. Comm. Pure Appl. Math. XVII (1964), 35–92.

[4] BRAMBLE J.H., PING LEE.: *On variational formulations for the Stokes equations with non-standard boundary conditions*. Mathematical Modelling and Numerical Analysis (1994), 28(7):903–919.

[5] BREZZI F.: *On the existence, uniqueness and approximation of saddle-point problems arising from Lagrange multipliers*. R.A.I.R.O., Anal. Numer. 8 (1974), 129–151.

[6] BREZZI, F., FORTIN, M.: *Hybrid and Mixed Finite Elements Methods*. Springer, N.Y. 1991.

[7] CHIZHONKOV, E.V.: *On the Constant in the LBB Condition for Ring Domains*. Department of Mathematics University of Nijmegen The Netherlands Report No. 9537 (1995).

[8] CROUZEIX, M.: *Étude d'une méthode de linéarisation. Résolution numérique des équations Stokes stationnaires*. In: Cahier de l'INRIA 12, pp. 139–244 (1974).

[9] CROUZEIX, M.: *On an operator related to the convergence of Uzawa's algorithm for the Stokes equation*. In: Computational Science for the 21st Century (Périaux, J., et al., eds. N.Y., Wiley 1997, 242–249.

[10] DOBROWOLSKI,M.: *A discrete solenoidal finite difference scheme for the numerical approximation of incompressible flows*. Numer. Math. 54 (1989), 533-542.

[11] DOBROWOLSKI, M., STOYAN, G.: *Algebraic and discrete Velte decompositions*. BIT 41, No. 3 (2001), 465–479.

[12] DOBROWOLSKI, M.: *On the LBB-Constant on Streched Domains*. Math.Nachr. 254-255 (2003) 64-67.

[13] FRIEDRICHS, K.O.: *On certain inequalities and characteristic value problems for analytic functions of two variables*. Trans. Amer. Math. Soc. 41, (1937), 321–364.

[14] GIRAULT V., RAVIART P.-A.: *Finite Element Methods for Navier-Stokes Equations*. Springer, Berlin 1986.

[15] GRIFFITHS,D.F.: *Finite elements for incompressible flow*. Math. Meth. in the Appl. Sci. 1 (1979), 16-31.

[16] HACKBUSCH, W.: *Multi-Grid Methods and Applications*. Springer-Verlag Berlin, Heidelberg 1985.

[17] HEINRICH B.: *Finite Difference Methods On Irregular Networks*. Akademie-Verlag, Berlin 1987.

[18] KRATZ W.: *The maximum modulus theorem for the Stokes system in a ball*. Mathematische Zeitschrift, 226, 389-403 (1997).

[19] LADYZHENSKAYA, O.A.: *Mathematical Theory of Viscous Incompressible Flow*. 2. ed., Gordon and Breach, New York 1969.

[20] LOPATINSKIJ, Y.B.: *On a method of reducing boundary problems for a system of differential equations of elliptic type to regular equations*. Ukrain. Mat. Zh. 5 (1953), 123–151.

[21] SCHLEGEL, M.: *Ergebnisse zur Lösung des Eigenwertproblems der nichtlinearen Stabilitätstheorie für Kanalströmungen*. Thesis, Universität Magdeburg (2002).

[22] STOYAN, G.: *Towards discrete Velte decompositions and narrow bounds for inf-sup constants*. Computers & Maths. with Appls., 38, 7-8 (1999), 243–261.

[23] STOYAN, G.: *Iterative Stokes solvers in the harmonic Velte subspace*. Computing 67 (2000), 13–33.

[24] STOYAN, G.: $-\Delta = -\operatorname{grad}\operatorname{div} + \operatorname{rot}\operatorname{rot}$ *for matrices, with application to the finite element solution of the Stokes problem*. East-West Journal of Numer. Math. 8,4 (2000), 323–340.

[25] STOYAN, G., STRAUBER, GY., BARAN, A.: *Generalizations to discrete and analytical Crouzeix-Velte decompositions*. Numer. Lin. Algebra with Appls., 11, (2004), 565–590.

[26] Stoyan, G., Takó G.: *Numerical Methods II.* Typotex Budapest (1995) (in Hungarian).

[27] Stoyan, G., Takó G.: *Numerical Methods III.* Typotex Budapest (1997) (in Hungarian).

[28] Strauber, Gy.: *Discrete Crouzeix-Velte decompositions on nonequidistant rectangular grids*. Annales Univ. Sci. Budapest.,44 (2002), 63-82.

[29] Strauber, Gy.: *Discrete Crouzeix-Velte decomposition for the disk domain.* Miskolc Mathematical Notes, Vol.6 (2005), No. 1, pp. 129-143.

[30] Varnhorn, W.: *The Stokes Equations*. Akademie Verlag, Berlin, 1994.

[31] Velte, W.: *On optimal constants in some inequalities. In: The Navier-Stokes Equations*; Theory and Numerical Methods (J.G. Heywood et al., eds.). Lecture Notes in Math. 1431, pp. 158–168. Berlin: Springer 1990.